



A novel GIS-based multicriteria analysis approach for ascertaining the catchment-scale degradation of a Himalayan wetland



Irfan Rashid^{a,*}, Sheikh Aneaus^a, Shahid Ahmad Dar^b, Ovaid Javed^a, Shabir Ahmad Khanday^b, Sami Ullah Bhat^b

^a Department of Geoinformatics, University of Kashmir, Hazratbal Srinagar, 190006, Jammu and Kashmir, India

^b Department of Environmental Science, University of Kashmir, Hazratbal Srinagar, 190006, Jammu and Kashmir, India

ARTICLE INFO

Handling Editor: Ajie Wang

Keywords:

Remote sensing
Geospatial analysis
Wetland health
Land system changes
Water quality analysis
Fragmentation
Soil erosion
Kashmir Himalaya

ABSTRACT

Wetland degradation through a diverse spectrum of anthropogenic stressors worldwide has taken a heavy toll on the health of wetlands. This study examined the health of a semi-urban wetland Bodas, located in the Kashmir Himalaya using multicriteria analysis approach assimilating data on land use land cover (LULC), landscape fragmentation, soil loss, and demography. Wetland and catchment-scale land system changes from 1980 to 2022 were assessed using high-resolution imagery. Fragmentation of the natural landscape was assessed using the Landscape Fragmentation Tool (LFT) and soil loss was assessed using the Revised Universal Soil Loss Equation (RUSLE). In addition, the water quality was examined at 12 sites distributed across the wetland using standard methods. Satellite data revealed 12 categories of land use with areas under exposed rock, orchards, built-up and sparse forest having increased by 1005%, 623%, 274%, and 37% respectively. LFT indicated that the core (>500 acres) and core (<250 acres) zones decreased by approximately 16% and 64%, respectively, whereas the areas under the perforated, edge and patch classes increased significantly. RUSLE estimates show a ~77% increase in soil erosion from 116.26 Mg a⁻¹ in 1980 to 205.68 Mg a⁻¹ in 2022, mostly due to changes in LULC. Total phosphorus (0.195–2.04 mg L⁻¹), nitrate nitrogen (0.306–2.79 mg L⁻¹), and total dissolved solids (543–774 mg L⁻¹) indicated nutrient enrichment of the wetland influenced by anthropogenically-driven land system changes. The wetland degradation index revealed that 21% of the wetland experienced high-to-severe degradation, 62% experienced moderate degradation, and 17% did not face any significant degradation pressure. The novel GIS-based approach adopted in this study can act as a prototype for ascertaining the catchment-scale degradation of wetlands worldwide.

1. Introduction

Wetland ecosystems are among the most vulnerable and exposed ecosystems in the world (Dar et al., 2022a). Wetlands support a wide range of biological diversity (Krina et al., 2020; Xu et al., 2020), and deliver goods and services with high ecological significance (Bassi et al., 2014; Borchert et al., 2018). They offer many economic and ecological benefits (Zhao et al., 2005), such as carbon sequestration (Lolu et al., 2020), groundwater recharge, flood absorption basins (Qiao et al., 2019), and food and fodder (Verhoeven and Setter, 2010), etc. Worldwide, wetlands face immense degradation pressure mostly due to anthropogenically-driven land system changes (Zedler and Kercher, 2005; Brinson and Malvárez, 2002; Karim et al., 2016). These include agriculture-intensive practices (Lin and Yu, 2018), urbanisation (Basu

et al., 2021; Mao et al., 2018), and the destruction of natural habitats (Song et al., 2021; Mantyka-pringle et al., 2012). Alterations in wetland catchments due to anthropogenically induced land use-land cover changes (LULCCs) alter the state of wetlands (Wu et al., 2013) by impacting various land surface processes (Wang et al., 2007; Romshoo et al., 2012). Changes in the landscapes surrounding pristine wetland ecosystems ultimately affect the function and cycling of nutrients (Liu et al., 2019; Sui et al., 2019).

The need to meet the increasing demand for land due to demographic pressures is pushing people to shift to less-congested areas, resulting in irreversible changes to landscapes (Dadashpoor and Ahani, 2021). Urbanisation, which is a significant land cover change, is responsible for decreased water retention and soil porosity, resulting in increased runoff and, in some cases, stormwater floods (Choi and Deal, 2008; Issa et al.,

* Corresponding author.

E-mail address: irfangis@kashmiruniversity.ac.in (I. Rashid).

2011). In this regard, the impact of LULCCs on surface processes, such as soil erosion and surface runoff, using physically-based geospatial models is growing (Rashid and Aneaus, 2019; Rashid et al., 2022b). There is considerable scientific evidence demonstrating the application of several erosion models at various spatiotemporal scales for numerical calculations and scenario-based simulations (Panagos et al., 2015; Eekhout et al., 2018; Shrestha and Jetten, 2018). Several empirical, process-based, and physical tools, such as the Water Erosion Prediction Project (WEPP) (Flanagan et al., 2013; Boll et al., 2015), RUSLE (Phinzi and Ngetar, 2019; Zhang et al., 2013), and Soil and Water Assessment Tool (SWAT) (Douglas-Mankin et al., 2010; Francesconi et al., 2016), have been used to quantify soil loss across wide topographic and climatic settings worldwide.

The improved spatial resolution of remote sensing data products (Leyk et al., 2019), availability of ancillary data (Pengra et al., 2020), and advancements in GIS methods have become fairly robust (Ban et al., 2020; Pratihast et al., 2016). Recent studies utilizing remote sensing and GIS methods have suggested massive land system changes across Kashmir Valley (Rashid et al., 2016, 2017a; Penny et al., 2022). LULCCs have harmed lakes and wetlands (Romshoo and Rashid, 2014; Dar et al., 2020a), which predominantly includes habitat loss of waterfowl (Alam et al., 2020), reduction in flood water storage (Romshoo et al., 2018; Pandit, 1988), and siltation (Rashid and Aneaus, 2019; Rashid et al., 2013). Additionally, the loss of forest cover (Haq et al., 2020) and overgrazing of pastures (Ahmad, 2013; Shaheen et al., 2017; Islam et al., 2021) in catchments result in soil erosion, which causes siltation and ultimately reduces the water depth of wetland ecosystems (Khan et al., 2004; Rather and Pandit, 2002).

In this context, it is imperative to link LULCCs, associated land surface processes, demography, and hydrochemistry to ascertain wetland health. The most plausible approach is to generate information on each of these factors using remote sensing methods, lab-based standard

analyses, field investigations, ancillary data repositories, and geospatial models that can then be integrated into a GIS environment to provide a clear picture of the contributing factors affecting wetland health. Such a rich database can contribute significantly to improving our understanding of the current degradation state of these ecosystems, which will help policymakers implement better strategies for sustainable management of wetland ecosystems. Therefore, this study aimed to ascertain the health of the Bodsar Wetland, located in the Kashmir Himalaya, India, from 1980 to 2022 through catchment-scale LULCCs, associated land cover fragmentation modelling, soil loss modelling, demographic changes, and water quality analysis.

2. Material and methods

2.1. Study area

Bodsar Wetland, also called Chatlam, is located on the semi-urban fringe of the Pampore area 15 km from the capital city of Srinagar. The wetland lies between the geographic coordinates of $74^{\circ}58' - 74^{\circ}59'$ E longitude and $34^{\circ}5' - 34^{\circ}46'$ N latitude at an altitude of 1599 amsl in the northmost Himalayan Union Territory of Jammu and Kashmir, India. The wetland covers an area of 0.51 km^2 , mostly comprising aquatic vegetation, marsh, and open water (Fig. 1). The wetland is a permanent, relatively shallow water body with a depth of 2.75 m (Raina, 1981). The wetland is bounded by smaller wetlands, namely Drangbal and Meej, and the catchment area is 200 km^2 , stretching from Pampore (west) to Wuyan and Konibal (east) (Paray et al., 2010). The source of the water that feeds the wetland (Ziarat Spring), was confirmed using the Survey of India Toposheet of 1962, which drains into the Jhelum River through an outlet channel. The wetland acts as a breeding and feeding ground for migratory birds including a variety of waterfowl species (Pandit, 1991; Fazili et al., 2017).

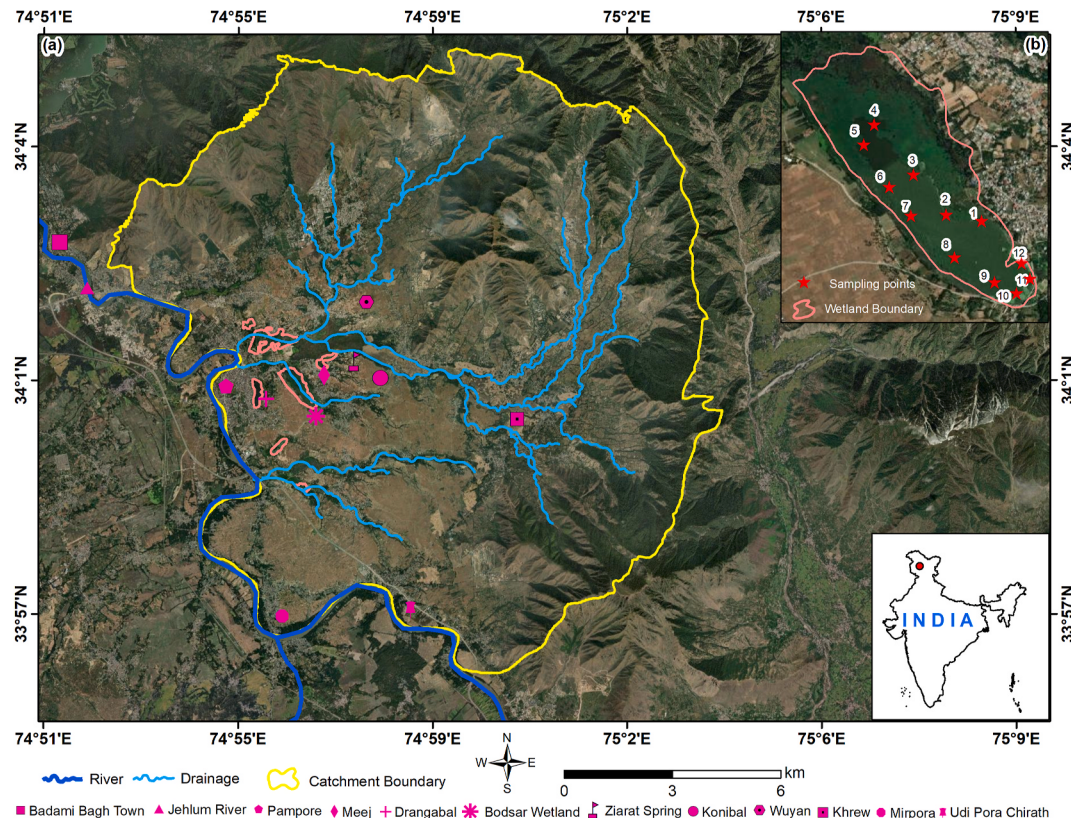


Fig. 1. Geographic domain of analysis showing wetlands, major drainage and important localities. Background image: High-Resolution Planetscope imagery dated 1 October 2022. Inset (top right): Location of water quality sites in the Bodsar wetland. Inset (bottom right): Location of the study area with respect to the Indian mainland.

2.2. Satellite data acquisition and LULC mapping

High-resolution satellite images (Table 1) were used to identify and delineate different LULC categories using various elements of image interpretation (Lillesand et al., 2015). The wetland boundary was delineated manually at a 1:50000 scale utilizing the Survey of India Toposheets surveyed in 1962. High-resolution CORONA image from 1980 and Google Basemap from 2022 were used for LULC mapping. The CORONA 1980 image was georeferenced and co-registered using “map-to-image and image-to-image” georeferencing to ensure the overlap of the 1980 and 2022 data in a GIS environment (Jensen, 2015). To assess catchment-scale LULCCs, ESRI ArcMap 10.2 was used to manually delineate different LULC categories at a scale of 1:3000. Various LULC classifications were defined following the Indian Space Research Organization’s National Natural Resources Management System (NNRMS) criteria (ISRO, 2005).

The Land Cover Index (LCI) was built on the existing LULC classes. The different land cover classes were assigned weights ranging from 1 to 4 based on their impacts on wetland degradation. A lower value of 1 was assigned to aquatic vegetation, open water and exposed rock classes; 2 to dense and sparse forest, bare soil, shrubland, plantation and pasture; 3 to built-up; and 4 to cropland and orchards in the wetland catchment. The weighted scheme is logical because the built-up areas and associated activities in the catchment are the most likely sources of nutrient load and siltation of the wetland.

2.3. Accuracy assessment

The precision of the 2022 LULC obtained from satellite data was assessed not only to prove the dependability of information but also to understand the mistakes and their anticipated repercussions (Hu et al., 2018). A random sampling approach was used to validate the lab-generated data by collecting data from 221 locations using the Trimble Juno SB Global Navigation Satellite System (GNSS) having an accuracy of ± 10 m. The overall and class accuracies were computed as suggested by Rashid et al. (2017a) as follows:

$$\rho = (n / N) \times 100$$

Table 1
Details of the datasets used to conduct this study.

Datasets	Specific dataset	Source	Acquisition date	Spatial resolution /Scale
Satellite data	Declassified Corona imagery	https://earthexplorer.usgs.gov/	7 October 1980	1.87 m (6 ft)
	Planetscope imagery	http://www.planet.com/	1 October 2022	3 m
Topographic data	SRTM DEM	https://earthexplorer.usgs.gov/	February 2000	30 m
Soil data	Soil Texture	Sheri Kashmir University of Agricultural Science and Technology (SKUAST), Srinagar	2010–2022	1:10 000
Meteorological data	WorldClim version 2	http://www.worldclim.org/	1970–2000	1 km
Field data	GPS measurements	Ground Survey	2019	Point data
	Water samples for physicochemical assessment	Ground Survey	2019	Point data

where ρ represents the accuracy, n represents the number of correctly categorised points in the image, and N denotes the total number of points collected throughout the ground truth campaign.

2.4. Demographic changes

Information on changing demography is crucial for linking stress in ecosystems to degradation on varying spatiotemporal scales (Mouri et al., 2011). We used population data at the village level to generate a demographic index and to relate the effects of a growing population to LULCCs. Demographic data for 1981, 2001, and 2011 were obtained from the Census of India. The data for 1991 and 2021 were projected using a second-order polynomial trend that fitted the population change and is described as follows:

$$y = 71.317x^2 - 281741x + 3 \times 10^8 \quad (1)$$

It is worth noting that the population census was not conducted in 1991 because of political disturbances in the Kashmir region (Varshney, 1991) whereas the 2021 census was delayed due to prevalent COVID-19 scenario. A population index (PI) was created based on the total number of inhabitants in the catchment area, which included three towns (Badami Bagh, Khrew, and Pampore) and 45 villages. The weights were assigned from 1 to 4 with ‘1’ assigned to a population ranging from 0 to 4000, ‘2’ to a population ranging from >4000 to 8000, ‘3’ to population ranging from >8000 to 16000 and ‘4’ to population ranging from >16000 to 26000.

2.5. Landscape fragmentation

LFT version 2.0, which allows users to analyse LULC raster layers, was used to estimate the extent of fragmentation that occurred over a course of time. The model can be downloaded from <https://clear.uconn.edu/projects/landscape/download/> and is used as an extension in ArcMap 10.2 or later versions. The LFT classifies different land cover features into four classes (core, perforated, edge, and patch), depending on the level of fragmentation in the landscape. Core zones are defined as zones that are essentially surrounded by forests and far from the boundary of non-forest pixels. The core zones were classified into two types based on the size of the patch and the edge effect: $core < 250$, and $core > 500$. Patch pixels are areas within a forest section that lack a core pixel. The edge and perforated pixels are located within 100 m of the urban pixels, although they are also included in the zone comprising the core pixels. The edge zone is near the outer edge of the forest zone whereas the perforated zone is adjacent to the edge of the forest zone. To estimate landscape fragmentation, LFT utilises information about forested and non-forested ranges. To ascertain landscape fragmentation over different periods, LULC information was reclassified into forested and non-forest categories. The natural land cover categories that include sparse forest, aquatic vegetation, pasture, dense forest, plantation, scrubland, and open water were reclassified as “forest” and the categories that include cropland, built-up, exposed rock, bare soil and orchard were reclassified as “non-forested”. This resulted in two fragmentation maps for 1980 and 2020, respectively.

The fragmentation index (FI) for the 2020 dataset was generated based on the fragmentation in the catchment area. Different classes were assigned weights ranging from 1 to 4 based on the level of fragmentation in the catchment due to various land use classes. The smallest weight of 1 was assigned to the least fragmented class, 2 to the perforated category, 3 to the edge category, and 4 to the patch category of fragmentation in the catchment.

2.6. Erosion modelling

RUSLE is an empirical model that uses data on rainfall patterns, soil type, topography, agricultural systems, and management techniques to

forecast the long-term mean annual rates of soil erosion (Renard et al., 1997). The model not only predicts soil erosion in unmeasured watershed features and local climatic and hydrological features but can also exhibit a spatial array of soil erosion (Angima et al., 2003; Pan and Wen, 2014). This implies that the model can be highly useful for predicting erosion at the catchment level (Fang et al., 2019). RUSLE calculates erosion of soil as follows:

$$A = R \times K \times LS \times C \times P \quad (2)$$

where A represents the mean yearly projected loss of soil from the sheet and reel method ($t \text{ ha}^{-1} \text{ a}^{-1}$), R represents the erosivity factor ($\text{MJ mm ha}^{-1} \text{ h}^{-1} \text{ a}^{-1}$), K is the erodibility of soil ($\text{Mg h MJ}^{-1} \text{ mm}^{-1}$), LS is the length of the slope and topographic/steepleness factor, C represents the crop management factor, and P represents support practices (dimensionless). Soil loss in the wetland catchment from 1980 to 2022 was computed using equation (2). The steps for generating input datasets for RUSLE are outlined below.

The R-factor is highly affected by the storm intensity, duration, and potential. Rainfall data obtained from WorldClim version 2 (<http://www.worldclim.com/version2>) was used for measurement of the R-factor for 1970–2000 since in-situ data is not available over the catchment (Hijmans et al., 2005). The rainfall dataset with a spatial resolution of $1 \text{ km} \times 1 \text{ km}$ was clipped for the wetland catchment. WorldClim provides meteorological data that has been extensively used in catchment-scale geospatial and other ecological models (Lavorel et al., 2017; Vega et al. 2017). The R-factor was measured using data from mean annual rainfall between 1980 and 2022 since there have not been any noteworthy changes in total precipitation patterns in the region (Rashid et al., 2015). The R-factor was derived by using a standard approach (Singh et al., 1981) as follows:

$$R_{fac} = 79 + 0.363R \quad (3)$$

where R_{fac} denotes rainfall erosivity, and R denotes the mean annual average rainfall in millimetres.

The K-factor is a measure of the soil particle sensitivity to detachment and transport by runoff (Panagos et al., 2014). Soil texture is a significant factor in assessing soil erodibility. Data from Sheri Kashmir University of Agricultural Science and Technology in Kashmir were used to generate soil texture information with a spatial resolution of 100 m . Finally, a soil erodibility map was created using the K values (Table S1 Supplementary Material) for different soil types following Stone (2012).

The LS-factor specifies that erosion increases with slope length and angle as derived from the Shuttle Radar Topography Mission (SRTM) digital elevation model (DEM) with 30 m resolution. LS-factor was calculated using the approach described by Mitasova et al. (2001) as follows:

$$LS = \left(\frac{l}{72.6} \right)^m (65.41 \sin^2 \beta + 45.56 \sin \beta + 0.065) \quad (4a)$$

where l is the aggregate length of the slope in meters, β is the downhill slope angle, and m is the slope-dependent variable.

The C-factor considers how crop management, crops, and land cover affect soil loss in comparison to bare areas (Kinnell, 2010). Vegetative soil cover plays an important role in protecting the topsoil from erosive processes (Saumer et al., 2010). Its values range from 0 (extremely high crop/cover shielding topsoil from erosion) to 1 (no effect of crop/cover and considerable soil loss relative to bare soil) (Saumer et al., 2010). The C-factor was assigned to different LULC categories as described by Patil et al. (2015).

The P-factor illustrates the impact of activities that reduce the rate of runoff and soil erosion (Stone and Hilborn, 2000). The values varied from 0 to 1, with 0 indicating very good anthropogenic resistance to erosion, and 1 indicating no resistance to anthropogenic erosion (Sheikh et al., 2011). The P-factor was calculated from slope and LULC information according to Kumar et al. (2014). The LULC-wise C and P factors

are listed in Table S2 (Supplementary Material).

The erosion index (EI) was generated based on the erosion in 2022. The assigned weights were divided into four classes ranging from 1 to 4, with 1 indicating the least erosion and 4 indicating the highest erosion; 1 was assigned to the erosion category which ranged up to 50 kg ha^{-1} followed by 2 which ranged from 50 to 300 kg ha^{-1} , 3 which ranged from 300 to 500 kg ha^{-1} and 4 which ranged from 500 to 1645 kg ha^{-1} .

2.7. Water quality assessment

The sampling sites for determining the water quality were carefully chosen by constructing a sampling fishnet of $100 \text{ m} \times 100 \text{ m}$ using the GIS software. A portable multi-parameter probe (PCS Testr 35) was used to perform on-the-spot measurements of water quality variables such as pH, EC, and TDS. Other water quality variables were evaluated in a laboratory setting using the standard protocol of the American Public Health Association (APHA, 2017) (Table S3 Supplementary Material). All the water quality variables were interpolated in a GIS environment to produce a seamless spatial distribution using the kriging method.

$$Z(s_0) = \sum_{i=1}^n \lambda_i z(s_i) \quad (4b)$$

where $z(s_i)$ represents the measured value at the i th site; λ_i represents an unknown weight for the calculated value at the i th location; s_0 represents the predicted site; and n represents the number of calculated values.

The water quality index (WQI) was calculated by averaging the values of nitrate-nitrogen (NN), ortho-phosphate phosphorous (OPP), and TDS. These three variables are regarded as crucial parameters for nutrient enrichment in lakes and wetlands (Finlay et al., 2013). The pixel-wise values of these variables yielded the WQI for each pixel of the wetland (Rashid et al., 2017b) as follows:

$$WQI = \frac{1}{3} \sum_{i=1}^n NN, OPP, TDS \quad (5)$$

The resultant water quality scores were classified into four classes ranging from 1 to 4 (1 being the least polluted pixel and 4 representing the most polluted/nutrient-enriched pixel).

2.8. Determination of degradation status (DS) of wetland catchment

The wetland DS was determined by relating the anthropogenic and biophysical parameters with the water quality parameters using multi-criteria analysis in Arc Map 10.2 (Rashid et al., 2017). To the degradation status of the wetland catchment, we developed a degradation index (DS) that includes the catchment-scale LCI, PI, EI and FI. These indices were combined to create a pixel-wise DS for the wetland catchment as follows:

$$DS = \frac{1}{4} \sum_{i=1}^n LCI_i + PI_i + EI_i + FI_i \quad (6)$$

Using equal intervals, the DS values were classified into four classes: Low, Medium, High and Severe degradation based on the approach suggested by Rashid et al. (2017a,b).

3. Results

3.1. LULCCs within wetland

The investigation of the LULC classes revealed that the spread of open water has increased from 0.05 km^2 in 1980 to 0.15 km^2 in 2022, which indicates an increase of water area by $\sim 200\%$. However, during the same period, aquatic vegetation cover decreased by approximately 22% (Fig. S1, Table S4 Supplementary Material). We also looked into the

2014 satellite image and observed that during the 2014 mega flood, the aquatic vegetation showed a significant decrease of ~51% from having an area of 0.43 km² in 1980 to 0.22 km² in 2014. Open water expanse increased by ~100% from 0.05 km² in 1980 to 0.26 km² in 2014. The LULCCs inside the wetland are shown in Fig. 3. The aquatic vegetation of the Bodas Wetland comprises *Typha angustata*, *Phragmites communis*, and *Trapa natans*. And there have been numerous unsuccessful encroachment attempts in the past few years around the wetland to convert some portion of the wetland into residential area (<https://www.greaterkashmir.com/todays-paper/eyeing-the-pampore-wetlands>).

3.2. Catchment-scale LULCCs

Using manual delineation, we identified 12 LULC classes from high-resolution images of 1980 and 2022 that include cropland, aquatic

vegetation, bare soil, built-up, dense forests, orchard, pasture, plantation, shrubland, sparse forests, exposed rock, and open water (Fig. 2). Over the 42 years from 1980 to 2022, catchment-scale LULCCs indicated that the exposed rock has increased by 1.91 km² (1005%), orchard by 18.76 km² (623%), built-up by 10.6 km² (274%), scrub by 0.81 km² (142%), plantation by 10.18 km² (109%), open water by 0.07 km² (100%), and sparse forest by 1.97 km² (37%). Whereas the area under bare soil decreased by 0.45 km² (41%), and cropland by 36.38 km² (38%). Moreover, aquatic vegetation and dense forest also decreased in area by 0.43 km² (31%) and 5.38 km² (~18%) respectively. The overall accuracy of the 2022 LULC data was 89%, and the class-specific accuracies are listed in Table 2. Analysis of the data revealed that urbanisation increased four-fold. Similar trends have been reported in previous studies (Badar et al., 2013a; Rashid et al., 2020; Dar et al., 2021a) for other wetland catchments in Kashmir Himalaya. The extent of exposed

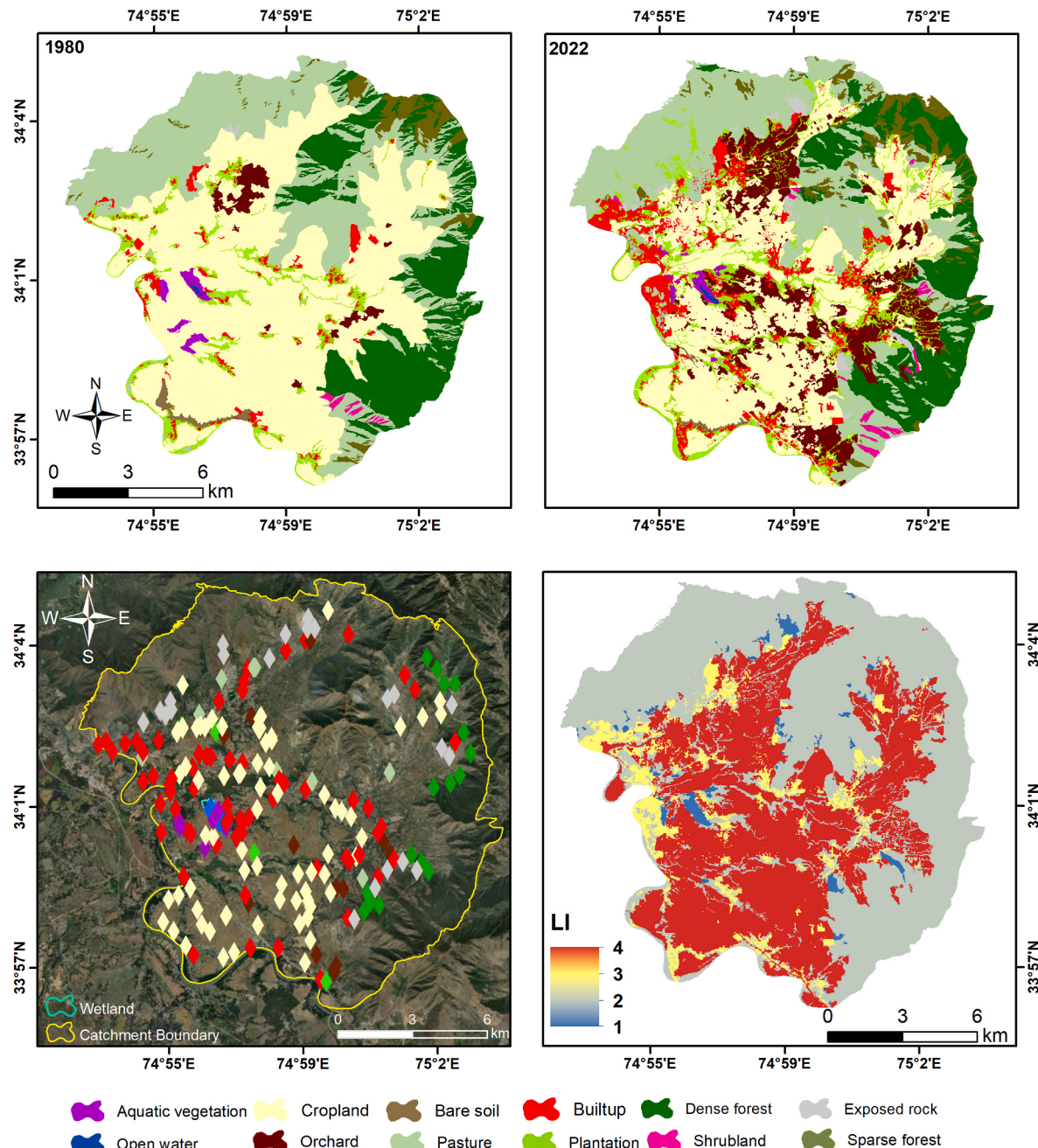


Fig. 2. Land system changes in the Bodas Wetland catchment from 1980 to 2022. Bottom left: Ground validation points for assessing the accuracy of 2022 land use land cover data. Bottom right: Land cover index derived from 2022 land use land cover data.

Table 2

LULC changes from 1980 to 2022 and accuracy assessment in the catchment of Bodsar wetland.

LULC Class	Area(km ²)		% change	Accuracy Assessment			
	1980	2022		n	N	p	
Crop Land	94.30	57.92	-36.38	-38.58	65	69	94
Aquatic Vegetation	1.37	0.94	-0.43	-31.39	4	5	80
Bare Soil	1.09	0.64	-0.45	-41.28	—	—	—
Built-up	3.87	14.47	10.6	273.90	55	67	82
Dense Forest	30.56	25.18	-5.38	-17.60	16	16	100
Exposed Rock	0.19	2.1	1.91	1005.26	22	22	100
Orchard	3.01	21.77	18.76	623.26	14	17	82
Open Water	0.07	0.14	0.07	100.00	12	12	100
Pasture	49.73	48.07	-1.66	-3.34	5	8	62
Plantation	9.33	19.51	10.18	109.11	4	5	80
Shrubland	0.57	1.38	0.81	142.11	—	—	—
Sparse Forest	5.31	7.28	1.97	37.10	—	—	—
				197	221	89.14	

rock tripled over the analysis period which is attributed to the various querying industries that have emerged in the area. This has led to increased erosion in the catchment area of the Bodsar Wetland, which is in agreement with the findings of [Ganaie et al. \(2021\)](#) for the Wular Lake catchment in Kashmir Valley.

3.3. Demographic changes

Information about the changing demography was analysed to determine the impacts of the growing population on land cover and the

environs around the Bodsar wetland. The total catchment population for 1981, 1991, 2001, 2011, and 2021 are 71723, 95000, 111549, 165504 and 220000 respectively ([Fig. 3](#)). In 1981, the highest population was observed in Badamibagh town (11227) followed by Wuyan village (3523) and the lowest population was observed in Udi Pora Chirath village (19). In 1991, the highest population in terms of town was forecasted to be Badamibagh town (15000) followed by Wuyan village (4600) and the lowest population was also forecasted in Udi Pora Chirath village (20). In 2001, the highest population was 18923 in Badamibagh, and the lowest was observed in Udi Pora Chirath village (21) of the Bodsar catchment. In 2011, the population statistics indicated a 17% (22214) increase in Badamibagh, and the lowest population was observed in Mirpora (12). For 2021, the population was predicted using a second-order polynomial trend, which predicted a significant increase in Badamibagh, Woyan and Udi Pora Chirath villages of 17% (26000), 2% (6000) and 159% (1500) respectively. The population density in the catchment for the year 1981 was 359 persons km⁻², for the year 1991 was 475 persons km⁻², for 2001 was 558 persons km⁻², for the year 2011 828 persons km⁻², and for the year 2021, it was predicted to be 1100 persons km⁻². The PI developed from population projections for 2021 suggests higher PI values for central, western and central east part of the wetland catchment.

3.4. Landscape fragmentation

Fragmentation analysis showed that in 1980 core>500 comprised approximately 86% of the total natural area ([Fig. 4, Table S5 Supplementary Material](#)) followed by edge (7%), core<250 (5%), patch (0.66%) and perforated (0.27%). In 2022 core >500 comprised

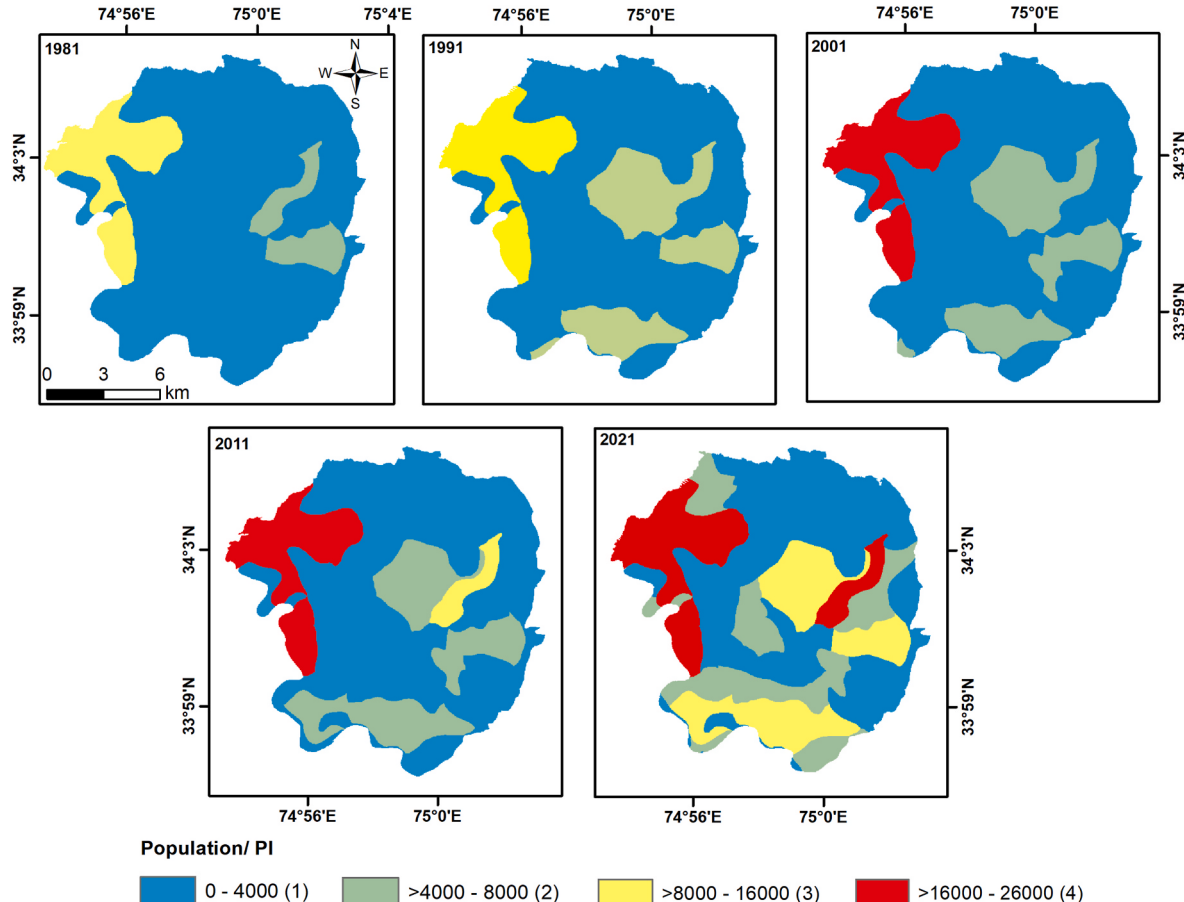


Fig. 3. Demographic changes in the catchment of the Bodsar wetland from 1981 to 2021. Bottom extreme right: Demographic index of the Bodsar wetland catchment derived from 2021 population data.

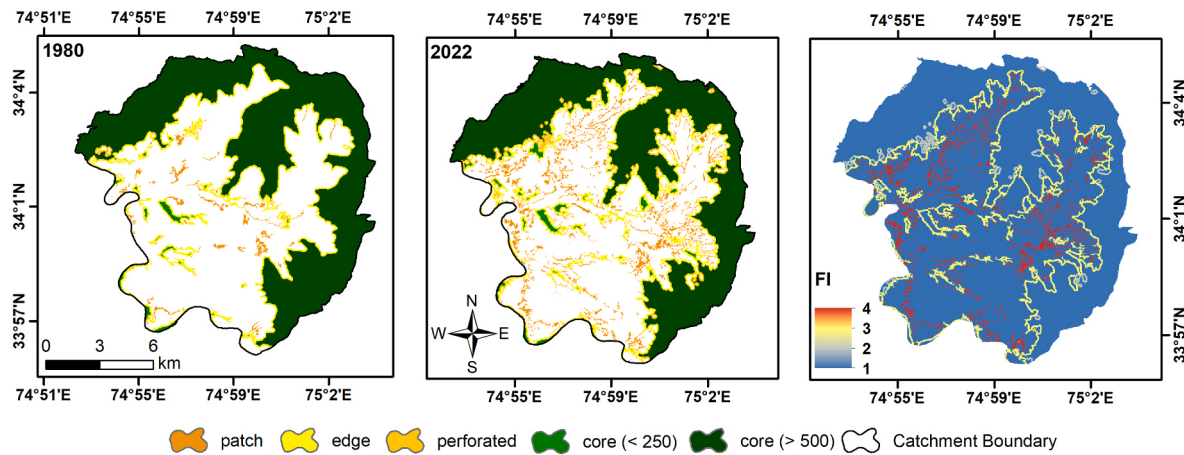


Fig. 4. Landscape fragmentation in the Bodsar wetland catchment derived from 1980 to 2022. Extreme right: Fragmentation index derived from 2022 land use land cover data.

approximately 68% of the natural area, edge (17%), patch (9%), core <250 (2%) and perforated (3%). According to this analysis, the core >500 area declined by $\sim 9 \text{ km}^2$ (16%) and the core <250 by 13.57 km^2 (64%). The area under the perforated class increased by 3.47 km^2 (1231%), that under the patch by approximately 10 km^2 (1425%) and that under the edge by 3 km^2 (147%).

3.5. Erosion estimations

Five vulnerability classes for soil erosion were identified: low (up to 50 kg ha^{-1}), moderate ($>50\text{--}150 \text{ kg ha}^{-1}$), high ($>150\text{--}300 \text{ kg ha}^{-1}$), very high ($>300\text{--}500 \text{ kg ha}^{-1}$), and severe ($>500\text{--}1645 \text{ kg ha}^{-1}$) (Fig. 5). For EI, very high and severe categories were merged together. Most of the wetland catchment falls under low to moderate-level erosion condition. High to very high erosion levels were also observed in areas under cropland and exposed rock land cover types which are attributed to lose soils that can detach easily compared to other land cover types. Very few pixels showed severe erosion due to steep slopes ranging from 7° to 7.9° . Our investigation showed that soil erosion in the Bodsar catchment increased considerably from 116.26 Mg a^{-1} in 1980 to

205.68 Mg a^{-1} in 2022. Soil loss from exposed rock indicated a massive increase of 105 kg ha^{-1} (1287%), sparse forest by $\sim 3 \text{ kg ha}^{-1}$ (72%), cropland by 0.58 kg ha^{-1} (1%), orchard by 27 kg ha^{-1} (38%) and bare soil by 5 kg ha^{-1} ($\sim 13\%$) from 1980 to 2022. Pasture and dense forests showed a decline in soil loss by 14 kg ha^{-1} (56%) and 0.5 kg ha^{-1} (23%) respectively which can be attributed to the plant cover that does not allow direct exposure to raindrops that accelerates detachment and removal of the soil layer. These data indicate that variability in LULC is one of the driving forces behind the changing soil erosion patterns in the study area.

3.6. Water quality analysis

The wetland water quality variables investigated at 12 sites (Fig. 1, Table 3) exhibited significant spatial variation (Fig. 6). The wetland water is neutral to slightly alkaline, with pH values ranging from 7 to 8.5. The EC varied between $765 \mu\text{S cm}^{-1}$ at site 7 and $1066 \mu\text{S cm}^{-1}$ at site 3. TDS levels were between 543 mg L^{-1} at site 7 and 774 mg L^{-1} at site 4. The TA concentration ranged from 132 mg L^{-1} at Site 9 to 160 mg L^{-1} at Sites 1 and 6. The total hardness values varied between 150 mg

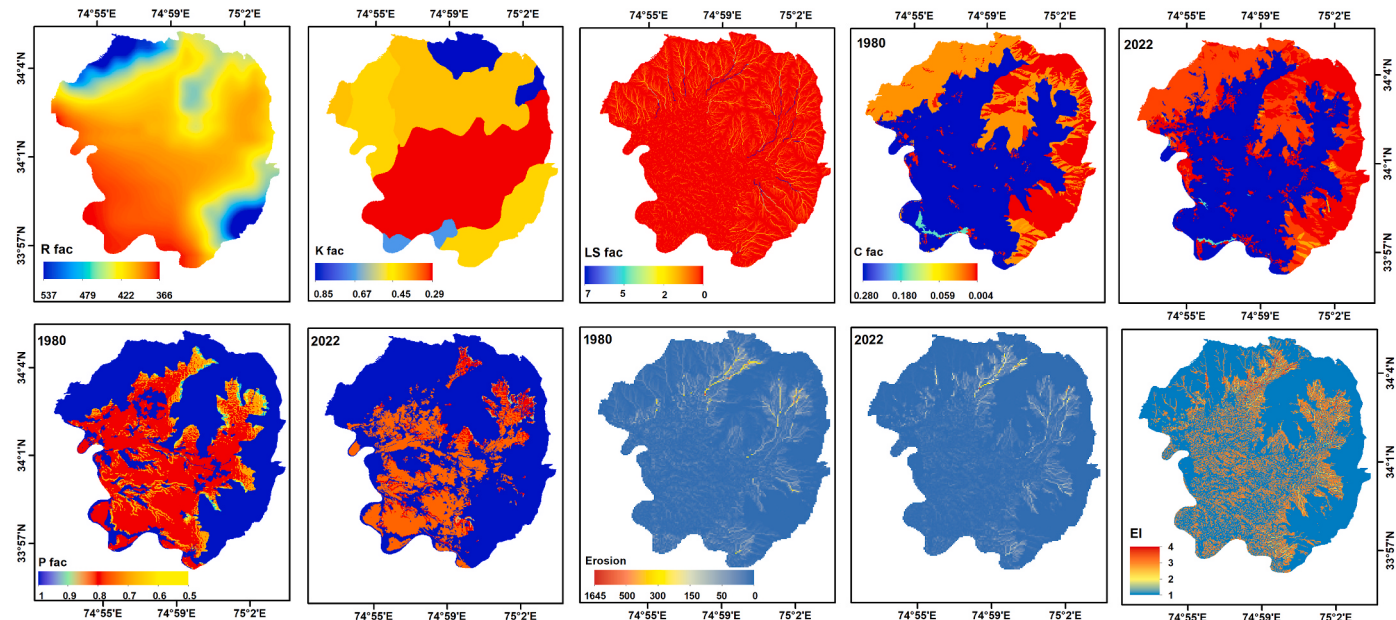


Fig. 5. Input parameters and erosion estimates from the RUSLE model for the Bodsar wetland catchment. Bottom extreme right: Erosion index derived from 2022 erosion data.

Table 3
Water quality analysis at 12 sites within Bodsar wetland.

Site No	pH	Conductivity ($\mu\text{s cm}^{-1}$)	TDS (mg L^{-1})	Total alkalinity (mg L^{-1})	Total hardness (mg L^{-1})	Calcium (mg L^{-1})	Magnesium (mg L^{-1})	Total Phosphorus (mg L^{-1})	Ortho Phosphorus (mg L^{-1})	Nitrate-N (mg L^{-1})	Ammoniacal-N (mg L^{-1})	Chloride (mg L^{-1})
Site 1	8.3	1050	734	160	180	58.9	18.9	2.04	0.992	2.79	0.812	52
Site 2	8.5	977	671	142	178	47.3	14.6	1.62	0.84	1.805	0.595	44
Site 3	8.1	1066	746	148	165	48.9	15.4	1.71	0.659	1.607	0.362	35
Site 4	7.8	963	774	138	156	44.9	10.7	0.982	0.388	1.24	0.179	42
Site 5	7.7	850	603	155	172	50.9	12.9	0.711	0.312	0.826	0.118	30
Site 6	8.1	828	587	160	184	56.1	13.7	0.945	0.426	0.985	0.127	36
Site 7	8.3	765	543	145	167	41.7	14.9	0.83	0.327	0.931	0.083	28
Site 8	8	985	699	140	154	44.1	10.7	0.702	0.271	0.849	0.069	32
Site 9	8.4	898	629	132	150	40.9	13.7	0.52	0.143	0.631	0.043	42
Site 10	8.5	864	604	152	170	49.7	11.2	0.195	0.131	0.306	0.026	38
Site 11	8.5	1008	705	148	182	52.1	15.6	0.317	0.145	0.544	0.052	40
Site 12	8.2	813	572	138	152	42.7	11.0	0.751	0.138	0.701	0.073	34

L^{-1} at Site 9 and 184 mg L^{-1} at Site 6. Calcium concentration varied from 40.9 mg L^{-1} at Site 9 to 58.9 mg L^{-1} at Site 1. Magnesium ranged from 10.7 mg L^{-1} at Sites 4 and 8 to 18.9 mg L^{-1} at Site 1. TP ranged from 0.1 mg L^{-1} at Site 10 to 2.0 mg L^{-1} at Site 1. Ortho-phosphate phosphorous (Ortho-P) ranged from 0.1 mg L^{-1} at Site 10 to 0.9 mg L^{-1} at Site 1. NO_3^- -N concentration ranged from 0.3 mg L^{-1} at Site 10 to 2.7 mg L^{-1} at Site 1. NH_3 -N ranged from 0.02 mg L^{-1} at Site 10 to 0.8 mg L^{-1} at Site 1. The Cl^- concentration varied between 28 mg L^{-1} at Site 7 and 52 mg L^{-1} at Site 1.

The water quality of the wetland from 1980 to 2007 was also analysed in terms of pH, EC, Total Alkalinity, Total Hardness, Chloride, and Nitrate Nitrogen from the published works of Raina (1981), and Raina et al. (2009), respectively (Fig. S2 Supplementary Material). A comparison of the water quality datasets with previous studies revealed that pH and EC did not vary significantly between 1980 and 2019. However, from 2007 to 2019, the total alkalinity decreased from 515 mg L^{-1} to 138 mg L^{-1} , while the total hardness decreased from 330 mg L^{-1} to 156 mg L^{-1} . The values of chloride (112 mg L^{-1}) and nitrate nitrogen (8.9 mg L^{-1}) in 2007 also decreased significantly to 42 mg L^{-1} and 1.2 mg L^{-1} respectively in 2019.

3.7. Degradation status of the wetland and catchment

Based on the dissolved solid values, the wetland area was classified into various degradation classes such as Low, Medium, High, and Severe (Fig. 7, Table S6 Supplementary Material). It was observed that $\sim 21\%$ of the wetland falls within the High to Severe degradation zone, which lies towards the southeastern portion of the wetland. 62% of the southwest side of the wetland falls under the medium degradation zone and 17% falls under the low degradation zone. This degradation can be attributed to untreated waste from orchards, croplands, and built-up areas around the wetland.

The wetland catchment area was divided into four categories using MCA approach based on land use, demography, erosion, and fragmentation information (Fig. 7, Table S6 Supplementary Material). It was observed that $\sim 24\%$ of the catchment area falls in the low degradation category located around the northeastern and southeastern areas of wetland catchment with a mean slope of 19° . 63% of the catchment falls under the medium and high degradation category mostly under the land cover of orchards and croplands around the central part of the catchment with an average slope of 5.8° . 13% of the catchment falls under the severe category which is influenced by highly concentrated urbanised areas with an average slope ranging between 3° and 3.9° . The demographic results indicate that the population has increased around Chatlam village which is in the vicinity of the wetland and is projected to have expanded by 11% by 2021. Population growth is often related to the rise in anthropogenic activities, which can be directly responsible for worsening the health of wetland. The observations from the fragmentation and erosion analysis indicated that human influence including horticultural practices, and querying in the upper areas of the catchment are driving forces for erosion, as well as the formation of perforation in the natural land cover classes, resulting in patch formation.

4. Discussion

During this analysis, substantial LULCCs were observed in the catchment of the Bodsar Wetland. Between 1980 and 2022, we observed an increment of 273% ($\sim 11 \text{ km}^2$) in the built-up area which resulted in shrinkage of the cropland area. Similar observations have been documented for various urban and semi-urban wetlands in this region (Ahmed et al., 2021; Rafiq et al., 2018; Rasool et al. 2021). The area under orchards increased by 623% (18.76 km^2) which could be attributed to a shift from irrigation-intensive agricultural land under paddies to apple orchards driven by economic benefits (Bhat et al., 2021; Meraj et al., 2022) and depleted stream flows in the region (Showqi et al., 2014; Rather et al., 2016; Rashid et al., 2020). Aquatic vegetation in the

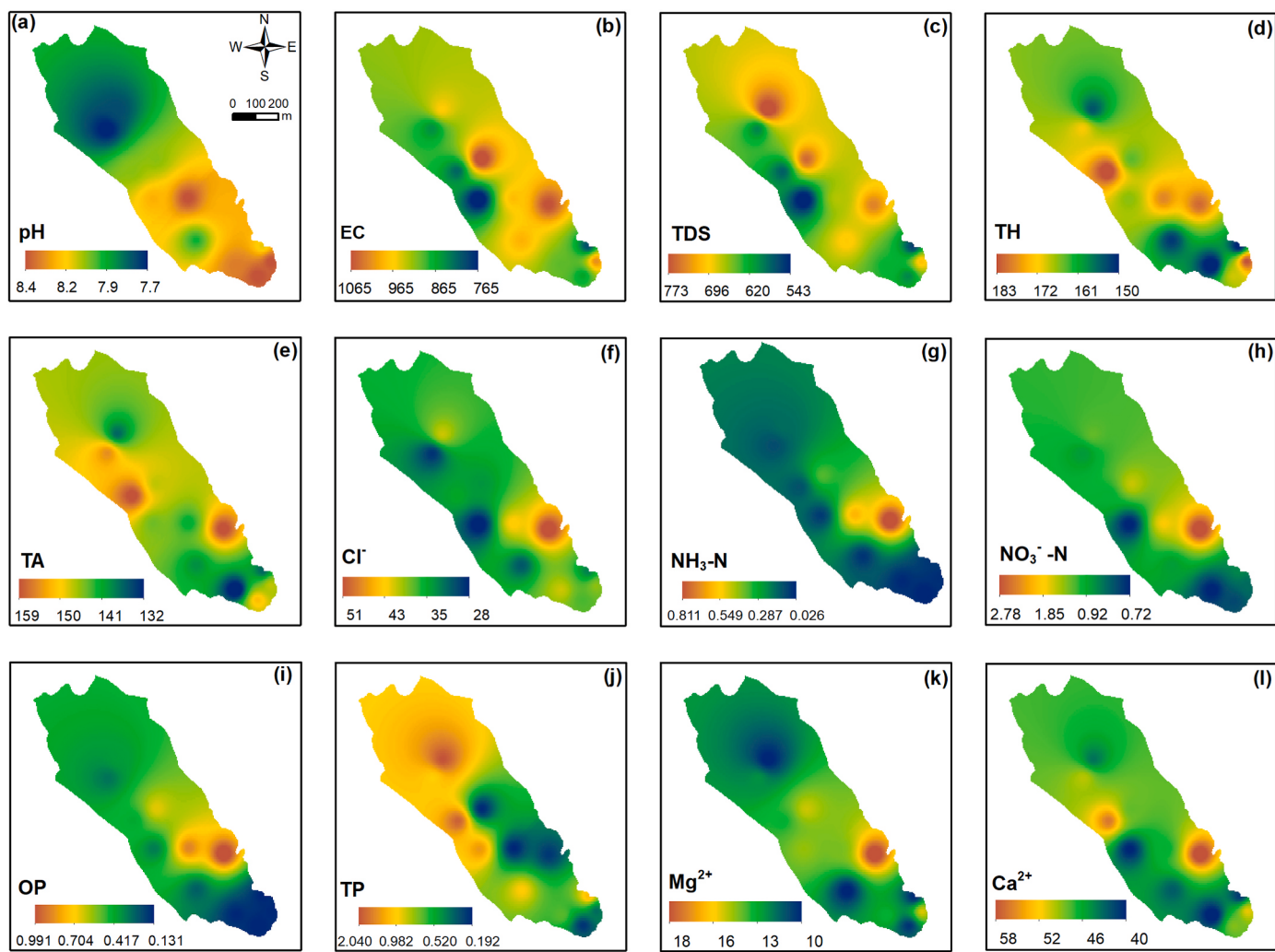


Fig. 6. Spatial variations in the water quality of the Bodsar wetland.

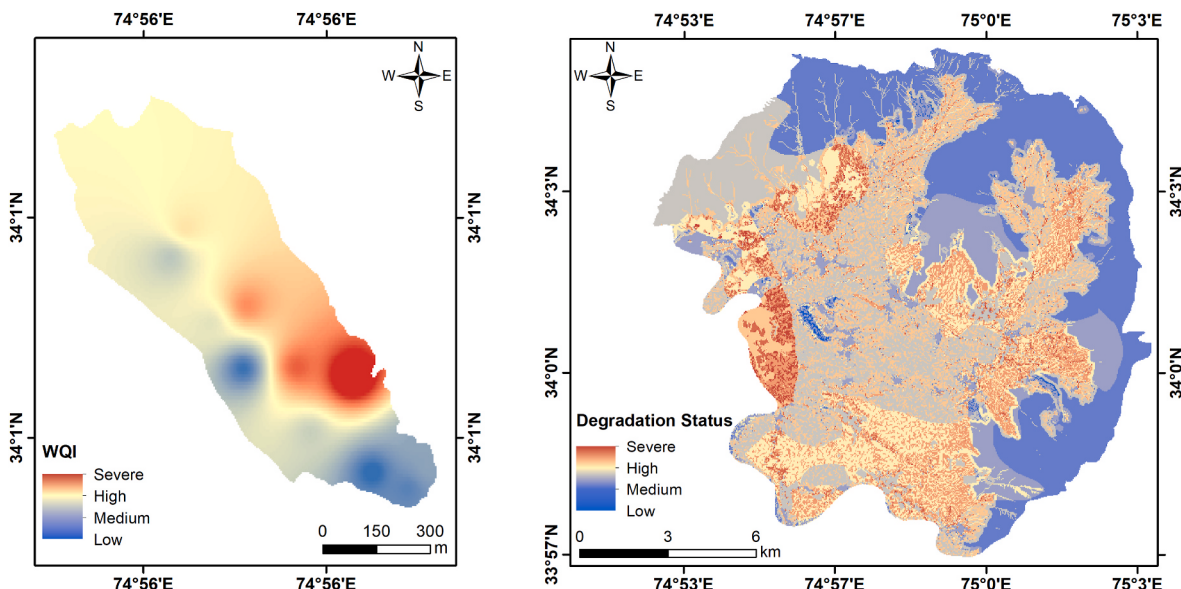


Fig. 7. Left: Water quality index of the Bodsar wetland. Right: Degradation index of Bodsar wetland catchment.

wetland has decreased by approximately 0.43 km^2 which can be attributed to various pressures such as siltation, algal bloom, changing land cover patterns, and global climate change (Dar et al., 2021b; Bakker et al., 2013). Notably, built-up areas increased in the Bodsar wetland catchment during the 42-year period, which could directly affect wetland nutrient influx, and enhance eutrophication, and sedimentation (Badar et al., 2013b; Amin et al., 2014). During the analysis, forest cover transformed from dense forest to sparse forest and shrubland, and the same findings were reported by Malik et al. (2017) for Kashmir Valley. This is attributed to increasing population pressure (Lone and Mayer, 2019), exploitation of fuelwood (Shaheen et al., 2016), and overgrazing (Haq et al., 2020) which hastens silt and nutrient supply in the catchment area (Ganaie et al., 2021). Such changes in the land system could hasten eutrophication of this wetland. The LCI revealed a significant human footprint in the catchment. LULCC is one of the largest indicators of human-induced changes at the catchment scale (Kindu et al., 2015). Changes in LULC together with other environmental factors such as topography and meteorology directly influence wetland degradation through soil erosion, nutrient leaching, etc (Sharma et al., 2011). The high rate of erosion from cropland and orchards in conjunction with the inputs of sewage into Bodsar has the potential to induce sedimentation of the wetland and hasten the cultural eutrophication (Vass et al., 2015), however, this needs to be researched further because we lack detailed time-varying bathymetry data of the wetlands in the region.

Demographic data of the village-wise human population from 1981 to 2021 were analysed. It was observed that there was a $\sim 207\%$ increase in population in the catchment of the Bodsar wetland. This was substantiated by the fact that built-up area increased by approximately 274% during the analysis period. Reports of population increase and urbanisation of wetland areas have also been reported in previous studies (Malik, 2012; Sajjad and Iqbal, 2012; Nengroo et al., 2017; Alam et al., 2020). Often, the rise in population is also associated with land-filling and encroachment in the vicinity of wetlands (Zaz and Romshoo, 2012). With the increasing human footprint, more densely populated areas have emerged, mostly around the western side of the wetland. This not only results in a decrease in the pervious area but also affects water quality and land surface processes (such as runoff generation, runoff peak time and increased frequency of stormwater floods) (Saraswat et al., 2016; Dar et al., 2022b; Yousuf and Romshoo, 2022). It is important to point out that the deterioration in water quality has already driven out *Botia birdi* and *Eurayle ferox* from most freshwater wetlands in Kashmir Valley. Nutrient enrichment has also caused the spread of invasive plant species in most aquatic ecosystems in the Kashmir Region (Bano et al., 2018). This, in turn, affects the community structure (Shah et al., 2021), food chain and associated food webs, nutrient and energy cycling, speed up the regime shift (Smol et al., 2005) and trophic status of lakes and wetlands (Mushtaq et al., 2022; Showqi et al., 2018). The DI correlates well with LCI inferring that there is a significant increase in the building footprint mostly around the proximity of the wetland on the northwest side also indicated a highly degraded water quality. Many researchers (Jia et al., 2015; Sun et al., 2017) have observed that ongoing population growth which includes infrastructural development is one of the major reasons for wetland degradation.

Habitat fragmentation includes the formation of smaller isolated patches of natural land cover and habitat loss. Since habitat loss harms biodiversity, researchers use fragmentation as a proxy to quantify habitat loss (Schmiegelow and Mönkkönen, 2002). In this study, the patch and perforated classes showed increases of $\sim 1400\%$, and $\sim 1230\%$, respectively, during the observation period. The area under the core- <250 also decreased by 64%. It is clear from the LULCCs that in the last five decades natural landscapes have been taken up by built-up areas, resulting in the fragmentation of otherwise vast land cover types. Similar trends have been observed in other urban settings across the Himalayas (Pandit et al., 2007; Reddy et al., 2013; Batar et al., 2017). The FI indicated that the collapsing of the natural landscape was mainly caused by demographic changes, increased building footprint as well as

the associated LULCCs (Sahana et al., 2018). This fragmentation can severely affect biotic and abiotic functions which have potential to degrade water quality (Debroy et al., 2022; Polgar and Jaafar, 2018; Shrestha et al., 2012).

The soil erosion estimates indicated an increase of 77% during the evaluation period. We observed large-scale urbanisation of the wetland catchment which could increase storm runoff and overland flow thereby increasing the sediment yield of the catchment (Jain and Das, 2010; Rashid and Aneaus, 2019; Wang et al., 2018). Associated land use practises such as quarrying has also increased by $\sim 517\%$ in the catchment from 0.06 km^2 in 2007 to 0.37 km^2 in 2022 (Fig. S3 Supplementary Material) forcing erosion in the catchment which was also indicated by EI. Quarrying not only causes erosion but also increases the particulate concentration in the atmospheric column which is a primary source of air pollution (Rashid et al., 2022a). This has negative impacts on human health, biodiversity, and water quality (Ganaie et al., 2018). Owing to the quarrying practices in the area the exposed rocks are constantly being excavated and vegetation is constantly being removed, which loosens the soil material and increases the silt load generated from the catchment, causing nutrient enrichment in the wetland (Paray and Koul, 2020; Rashid et al., 2013).

The higher EC and TDS concentrations recorded in the wetland are attributed to the addition of sewage, fertiliser runoff, and sediment loading from the horticultural and built-up areas in the wetland catchment. Similar observations were documented by Parvez and Bhat (2014) while working on Dal Lake in Kashmir Himalaya. The wetland's high Cl^- level implies the presence of organic materials, pollution, and sewage flow (Bhat and Pandit, 2014). $\text{NH}_3\text{-N}$ was discovered to be the main type of nitrogen in the wetland among other nitrogen species, and is associated with sewage inflow from adjacent built-up regions. Dar et al. (2021c) also reported $\text{NH}_3\text{-N}$ as the dominant form of nitrogen species in the Khushalsar wetland in Kashmir Valley. The TP concentration in the wetland is a matter of concern for wetland health as it has crossed the limit of hyper-eutrophication which is $100 \mu\text{g L}^{-1}$ (OECD, 2014).

The WQI reflected the state of water quality of the wetland. The wetland's high and severely deteriorated zones (21%) are closely associated with orchards and built-up areas. Dar et al. (2020b) and Qadir and Yousuf (2007) observed similar trends in neighbouring lakes and wetlands of the Kashmir Valley. It is important to mention that there is no Sewage Treatment Plant (STP) around the wetland that can treat the effluent sewage and runoff from built-up areas, agricultural lands and orchards before entering the Bodsar wetland.

The DS reflects anthropogenic interference in the wetland catchment. The GIS-based multi-criteria approach indicates that 62% of the catchment falls under medium and 21% under high degradation levels characterised by densely populated areas, agricultural lands and orchards demonstrating their strong influence on the degradation of the wetland. It is anticipated that the findings of this study will improve our understanding of the current ecological status of the wetland and identify various factors that have led to its degradation so that scientifically robust conservation strategies are framed based on this important knowledge base to fully restore the ecological and hydrological functionalities of the wetland.

Several studies worldwide have used a degradation index to assess wetland health. However, considering the use of environmental attributes, most studies have used only limited set of parameters that undermine catchment-scale interferences. The degradation index generated in this study is novel and improved because it is based on multisource information pertaining to land system, demography, erosion, landscape fragmentation, and water quality. The catchment-scale degradation indices generated in previous studies do not hold much ground owing to the lesser number of parameters used. For instance, Wanda et al. (2016) determined the risk assessment index of Lunyangwa Wetland, Malawi using the water quality and physical characteristics of the wetland. Lamsal et al. (2019) used information about land use, climate, and population to assess wetland changes in

Ghodaghodi Lake Complex, Nepal. [Shen et al. \(2019\)](#) studied 4 catchments in Zoige Plateau wetland in China from 2000 to 2015 using land use, fragmentation, and above ground biomass. In the Indian region, [Singh and Sinha \(2021\)](#) generated a catchment-scale wetland health index for the Kaabar Tal Wetland using hydrodynamics, geomorphic signatures, and vegetation information from 1976 to 2016. In the Kashmir Himalaya, [Badar et al. \(2013b\)](#) assessed the degradation status of Dal Lake catchment using only three attributes that include land use, soil, and population data. Similarly, [Rashid et al. \(2017a,b\)](#) assessed the degradation status of the Dal Lake ecosystem using the land use, population, and water quality data. [Dar et al. \(2021b\)](#) assessed the trophic state index of the Khushalsar Wetland using only water quality and LULC data. All of this points to the fact that these studies either focused on wetlands or were information-deficient when it comes to robust catchment-scale assessments. Therefore, the degradation index generated in this study is robust as it incorporates data from various influencing factors that are critical for wetland health. The GIS-based data integration used in this study is more flexible and can be improved by assimilating other information related to soil, geology and hydrometeorology.

5. Conclusion

This multi-proxy study utilizing information about land system, erosion, landscape fragmentation, demography and water quality indicated that the anthropogenic interferences has placed enormous pressure on the catchment of Bodsar wetland, resulting in its degradation. The anthropogenically driven land system changes in the last 4 decades have replaced the natural land cover resulting in fragmentation and increased soil loss. Intensive agricultural practices and untreated sewage ingress in the wetland have deteriorated water quality affecting not only the resilience of Bodsar wetland. The increased soil loss from the catchment would affect flood storage capacity and species composition of the Bodsar Wetland in the long term. This study demonstrates that human-induced LULCCs (increase in area under built up and orchards, decrease in cropland area and forest cover) and population increase affect the Bodsar Wetland. However, the wetland can be conserved through collaboration among stakeholders such as government officials, wetland managers, academia, NGOs, and local populations. With a flexibility to assimilate more data pertaining to the hydrology, soil moisture, soil biogeochemistry, and climate, we reiterate that this GIS-based MCA approach could be improved for identifying and characterising the catchment-scale degradation of wetlands worldwide.

Credit author statement

Irfan Rashid: Conceptualization, Supervision, Writing – original draft, Methodology, Investigation, Writing-Review and Editing. **Sheikh Aneaus:** Formal analysis, Methodology, Investigation, Writing – original draft. **Shahid Ahmad Dar:** Methodology, Investigation, Writing-Review and Editing. **Ovaid Javed:** Formal analysis, Investigation. **Shabir Ahmad Khanday:** Formal Analysis, Writing-Review and Editing. **Sami Ullah Bhat:** Conceptualization, Writing-Review and Editing.

Declaration of competing interest

The authors declare that they have no known competing financial interests or personal relationships that could have appeared to influence the work reported in this paper.

Data availability

The data generated in the research is available with the article

Acknowledgements

The authors thank the United States Geological Survey and Planet Labs PBC for freely providing the declassified satellite data and Planetscope images used in this research. The authors are grateful to the constructive comments of the three anonymous reviewers and Associate Editor-in-Chief, Prof. Ajie Wang, for handling and processing the manuscript.

Appendix A. Supplementary data

Supplementary data to this article can be found online at <https://doi.org/10.1016/j.envres.2023.115967>.

References

- Ahmad, S., 2013. Impact of varying disturbances on the structure and composition of grassland vegetation in Anantnag, Kashmir Himalayas. *Proc. Int. Acad. Ecol. Environ. Sci.* 3 (3), 219.
- Ahmed, R., Ahmad, S.T., Wani, G.F., Ahmed, P., Mir, A.A., Singh, A., 2021. Analysis of landuse and landcover changes in Kashmir valley, India-a review. *GeoJournal* 87, 4391–4403. <https://doi.org/10.1007/s10708-021-10465-8>.
- Alam, A., Bhat, M.S., Maheen, M., 2020. Using Landsat satellite data for assessing the land use and land cover change in Kashmir valley. *GeoJournal* 85, 1529–1543. <https://doi.org/10.1007/s10708-019-10037-x>.
- American Public Health Association (APHA), 2017. *Standard Methods for the Examination of Water and Waste Water*, 23rd Edition (Washington, USA).
- Amin, A., Fazal, S., Mujtaba, A., Singh, S.K., 2014. Effects of land transformation on water quality of Dal Lake, Srinagar, India. *J. Indian Soc. Remote Sens.* 42 (1), 119–128. <https://doi.org/10.1007/s12524-013-0297-9>.
- Angima, S.D., Stott, D.E., O'neill, M.K., Ong, C.K., Weesies, G.A., 2003. Soil erosion prediction using RUSLE for central Kenyan highland conditions. *Agric., Ecosyst. Environ.* 97, 295–308. [https://doi.org/10.1016/S0167-8809\(03\)00011-2](https://doi.org/10.1016/S0167-8809(03)00011-2).
- Badar, B., Romshoo, S.A., Khan, M.A., 2013a. Integrating biophysical and socioeconomic information for prioritizing watersheds in a Kashmir Himalayan lake: a remote sensing and GIS approach. *Environ. Monit. Assess.* 185, 6419–6445. <https://doi.org/10.1007/s10661-012-3035-9>.
- Badar, B., Romshoo, S.A., Khan, M.A., 2013b. Modelling catchment hydrological responses in a Himalayan Lake as a function of changing land use and land cover. *J. Earth Syst. Sci.* 122, 433–449. <https://doi.org/10.1007/s12040-013-0285-z>.
- Bakker, E.S., Sarneel, J.M., Gulati, R.D., Liu, Z., van Donk, E., 2013. Restoring macrophyte diversity in shallow temperate lakes: biotic versus abiotic constraints. *Hydrobiologia* 710, 23–37. <https://doi.org/10.1007/s10750-012-1142-9>.
- Ban, Y., Zhang, P., Nascetti, A., Bevington, A.R., Wulder, M.A., 2020. Near real-time wildfire progression monitoring with Sentinel-1 SAR time series and deep learning. *Sci. Rep.* 10 (1322) <https://doi.org/10.1038/s41598-019-56967-x>.
- Bano, H., Lone, F.A., Bhat, J.I., Rather, R.A., Malik, S., Bhat, M.A., 2018. Hokarsar Wet Land of Kashmir: its utility and factors responsible for its degradation. *Plant Arch.* 18, 1905–1910. [http://www.plantarchives.org/18-02/1905-1910%20\(4257\).pdf](http://www.plantarchives.org/18-02/1905-1910%20(4257).pdf).
- Bassi, N., Kumar, M.D., Sharma, A., Pardha-Saradhi, P., 2014. Status of wetlands in India: a review of extent, ecosystem benefits, threats and management strategies. *J. Hydrol.* Reg. Stud. 2, 1–19. <https://doi.org/10.1016/j.ejrh.2014.07.001>.
- Basu, T., Das, A., Pham, Q.B., Al-Ansari, N., Linh, N.T.T., Lagerwall, G., 2021. Development of an integrated peri-urban wetland degradation assessment approach for the Chatra Wetland in eastern India. *Sci. Rep.* 11 (4470) <https://doi.org/10.1038/s41598-021-83512-6>.
- Batar, A.K., Watanabe, T., Kumar, A., 2017. Assessment of land-use/land-cover change and forest fragmentation in the Garhwal Himalayan Region of India. *Environments* 34. <https://doi.org/10.3390/environments4020034>, 4(2).
- Bhat, S.A., Pandit, A.K., 2014. Surface water quality assessment of Wular Lake, A Ramsar site in Kashmir Himalaya, using discriminant analysis and WQI. *J. Ecosyst.* 724728. <https://doi.org/10.1155/2014/724728>.
- Bhat, M.S., Lone, F.A., Rather, J.A., 2021. Evaluation of long term trends in apple cultivation and its productivity in Jammu and Kashmir from 1975 to 2015. *GeoJournal* 86, 1193–1202. <https://doi.org/10.1007/s10708-019-10112-3>.
- Boll, J., Brooks, E.S., Crabtree, B., Dun, S., Steenhuis, T.S., 2015. Variable source area hydrology modeling with the water erosion prediction project model. *JAWRA J. Am. Water Resour. Assoc.* 51, 330–342. <https://doi.org/10.1111/1752-1688.12294>.
- Borchert, S.M., Osland, M.J., Enwright, N.M., Griffith, K.T., 2018. Coastal wetland adaptation to sea level rise: quantifying potential for landward migration and coastal squeeze. *J. Appl. Ecol.* 55, 2876–2887. <https://doi.org/10.1111/1365-2664.13169>.
- Brinson, M.M., Malvárez, A.I., 2002. Temperate freshwater wetlands: types, status, and threats. *Environ. Conserv.* 29, 115–133. <https://doi.org/10.1017/S0376892902000085>.
- Choi, W., Deal, B.M., 2008. Assessing hydrological impact of potential land use change through hydrological and land use change modeling for the Kishwaukee River basin (USA). *J. Environ. Manage.* 88, 1119–1130. <https://doi.org/10.1016/j.jenvman.2007.06.001>.
- Dadashpoor, H., Ahani, S., 2021. Explaining objective forces, driving forces, and causal mechanisms affecting the formation and expansion of the peri-urban areas: a critical

- realism approach. *Land Use Pol.* 102 (105232) <https://doi.org/10.1016/j.landusepol.2020.105232>.
- Dar, S.A., Bhat, S.U., Rashid, I., Dar, S.A., 2020a. Current status of wetlands in Srinagar City: threats, management strategies, and future perspectives. *Front. Environ. Sci.* 7 (199) <https://doi.org/10.3389/fenvs.2019.00199>.
- Dar, S.A., Bhat, S.U., Aneaus, S., Rashid, I., 2020b. A geospatial approach for limnological characterization of Nigeen Lake, Kashmir Himalaya. *Environ. Monit. Assess.* 192 (121) <https://doi.org/10.1007/s10661-020-8091-y>.
- Dar, S.A., Bhat, S.U., Rashid, I., 2021a. Landscape transformations, morphometry, and trophic status of Anchar Wetland in Kashmir Himalaya: implications for urban wetland management. *Water, Air, Soil Pollut.* 232 (462) <https://doi.org/10.1007/s11270-021-05416-5>.
- Dar, S.A., Rashid, I., Bhat, S.U., 2021b. Linking land system changes (1980–2017) with the trophic status of an urban wetland: implications for wetland management. *Environ. Monit. Assess.* 193 (710) <https://doi.org/10.1007/s10661-021-09476-2>.
- Dar, S.A., Rashid, I., Bhat, S.U., 2021c. Land system transformations govern the trophic status of an urban wetland ecosystem: perspectives from remote sensing and water quality analysis. *Land Degrad. Dev.* 32, 4087–4104. <https://doi.org/10.1002/lrd.3924>.
- Dar, S.A., Bhat, S.U., Rashid, I., Kumar, P., Sharma, R., Aneaus, S., 2022a. Deciphering the source contribution of organic matter accumulation in an urban wetland ecosystem. *Land Degrad. Dev.* 33, 2390–2404. <https://doi.org/10.1002/lrd.4280>.
- Dar, S.A., Hamid, A., Rashid, I., Bhat, S.U., 2022b. Identification of anthropogenic contribution to wetland degradation: insights from the environmetric techniques. *Stoch. Environ. Res. Risk Assess.* 36, 1397–1411. <https://doi.org/10.1007/s00477-021-02121-x>.
- Debroy, A., George, N., Mukherjee, G., 2022. Role of biofilms in the degradation of microplastics in aquatic environments. *J. Chem. Technol. Biotechnol.* 97, 3271–3282. <https://doi.org/10.1002/jctb.6978>.
- Douglas-Mankin, K.R., Srinivasan, R., Arnold, J.G., 2010. Soil and water assessment tool (SWAT) model: current developments and applications. *Trans. ASABE* 53, 1423–1431. <https://doi.org/10.13031/2013.34915>.
- Eckhout, J.P., Terink, W., de Vente, J., 2018. Assessing the large-scale impacts of environmental change using a coupled hydrology and soil erosion model. *Earth Surf. Dyn.* 6, 687–703. <https://doi.org/10.5194/esurf-6-687-2018>.
- Fang, G., Yuan, T., Zhang, Y., Wen, X., Lin, R., 2019. Integrated study on soil erosion using RUSLE and GIS in Yangtze river Basin of Jiangsu Province (China). *Arab. J. Geosci.* 12 173. <https://doi.org/10.1007/s12517-019-4331-2>.
- Fazili, M.F., Bhat, B.A., Ahangar, F.A., 2017. Avian diversity of Anchar lake, Kashmir, India. *New York Sci.* 10, 92–97. http://www.sciencepub.net/newyork/ny10011_7/15_31593nsy100117_92_97.pdf.
- Finlay, J.C., Smale, G.E., Sternier, R.W., 2013. Human influences on nitrogen removal in lakes. *Science* 342, 247–250. <https://doi.org/10.1126/science.1242575>.
- Flanagan, D.C., Frankenberger, J.R., Cochrane, T.A., Renschler, C.S., Elliot, W.J., 2013. Geospatial application of the water erosion prediction project (WEPP) model. *Trans. ASABE* 56, 591–601. <https://doi.org/10.13031/2013.42681>.
- Francesconi, W., Srinivasan, R., Pérez-Minana, E., Willcock, S.P., Quintero, M., 2016. Using the Soil and Water Assessment Tool (SWAT) to model ecosystem services: a systematic review. *J. Hydrol.* 535, 625–636. <https://doi.org/10.1016/j.jhydrol.2016.01.034>.
- Ganaie, T.A., Sahana, M., Hashia, H., 2018. Assessing and monitoring the human influence on water quality in response to land transformation within Wular environs of Kashmir Valley. *GeoJournal* 83, 1091–1113. <https://doi.org/10.1007/s10708-017-9822-7>.
- Ganaie, T.A., Jamal, S., Ahmad, W.S., 2021. Changing land use/land cover patterns and growing human population in Wular catchment of Kashmir Valley, India. *GeoJournal* 86, 1589–1606. <https://doi.org/10.1007/s10708-020-10146-y>.
- Haq, S.M., Khuroo, A.A., Malik, A.H., Rashid, I., Ahmad, R., Hamid, M., Dar, G.H., 2020. Biodiversity of the Himalaya: Jammu and Kashmir State. In: *Forest Ecosystems of Jammu and Kashmir State*. Springer, Singapore, pp. 191–208. https://doi.org/10.1007/978-981-32-9174-4_8.
- Hijmans, R.J., Cameron, S.E., Parra, J.L., Jones, P.G., Jarvis, A., 2005. Very high resolution interpolated climate surfaces for global land areas. *Int. J. Climatol.* 25, 1965–1978. <https://doi.org/10.1002/joc.1276>.
- Hu, T., Liu, J., Zheng, G., Li, Y., Xie, B., 2018. Quantitative assessment of urban wetland dynamics using high spatial resolution satellite imagery between 2000 and 2013. *Sci. Rep.* 8, 7409 <https://doi.org/10.1038/s41598-018-25823-9>.
- Islam, S.T., Dar, S.A., Sofi, M.S., Bhat, S.U., Sabha, I., Hamid, A., Jehangir, A., Bhat, A.A., 2021. Limnochemistry and Plankton diversity in some high altitude lakes of Kashmir Himalaya. *Front. Environ. Sci.* 9, 681965. <https://doi.org/10.3389/fenvs.2021.681965>.
- ISRO, 2005. **NNRMS standards: a national standard for EO images, thematic and cartographic maps, GIS databases and spatial outputs.** ISRO NNRMS Tech Rep No 112, 235.
- Issa, O.M., Valentin, C., Rajot, J.L., Cerdan, O., Desprats, J.F., Bouchet, T., 2011. Runoff generation fostered by physical and biological crusts in semi-arid sandy soils. *Geoderma* 167, 22–29. <https://doi.org/10.1016/j.geoderma.2011.09.013>.
- Jain, M.K., Das, D., 2010. Estimation of sediment yield and areas of soil erosion and deposition for watershed prioritization using GIS and remote sensing. *Water Resour. Manag.* 24, 2091–2112. <https://doi.org/10.1007/s11269-009-9540-0>.
- Jensen, J.R., 2015. One Lake Street Upper Saddle River, NJ United States. In: *Introductory Digital Image Processing: a Remote Sensing Perspective*. Prentice Hall Press.
- Jia, H., Pan, D., Zhang, W., 2015. Health assessment of wetland ecosystems in the Heilongjiang river Basin, China. *Wetlands* 35, 1185–1200. <https://doi.org/10.1007/s13157-015-0705-8>.
- Karim, F., Petheram, C., Marvanek, S., Ticehurst, C., Wallace, J., Hasan, M., 2016. Impact of climate change on floodplain inundation and hydrological connectivity between wetlands and rivers in a tropical river catchment. *Hydrol. Process.* 30, 1574–1593. <https://doi.org/10.1002/hyp.10714>.
- Khan, M.A., Shah, M.A., Mir, S.S., Bashir, S., 2004. The environmental status of a Kashmir Himalayan wetland game reserve: aquatic plant communities and eco-restoration measures. *Lakes & Reservoirs: Res. Manag.* 9, 125–132. <https://doi.org/10.1111/j.1440-1770.2004.00242.x>.
- Kindu, M., Schneider, T., Teketay, D., Knoke, T., 2015. Drivers of land use/land cover changes in Munessa-Shashemene landscape of the south-central highlands of Ethiopia. *Environ. Monit. Assess.* 187 (452) <https://doi.org/10.1007/s10661-015-4671-7>.
- Kinnell, P.I.A., 2010. Event soil loss, runoff and the Universal Soil Loss Equation family of models: a review. *J. Hydrol.* 385, 384–397. <https://doi.org/10.1016/j.jhydrol.2010.01.024>.
- Krina, A., Xystrakis, F., Karantinis, K., Koutsias, N., 2020. Monitoring and projecting land use/land cover changes of eleven large deltaic areas in Greece from 1945 onwards. *Rem. Sens.* 12 (1241) <https://doi.org/10.3390/rs12081241>.
- Kumar, A., Devi, M., Deshmukh, B., 2014. Integrated remote sensing and geographic information system based RUSLE modelling for estimation of soil loss in western Himalaya, India. *Water Resour. Manag.* 28, 3307–3317. <https://doi.org/10.1007/s11269-014-0680-5>.
- Lamsal, P., Atreya, K., Ghosh, M.K., Pant, K.P., 2019. Effects of population, land cover change, and climatic variability on wetland resource degradation in a Ramsar listed Ghodaghodi Lake Complex, Nepal. *Environ. Monit. Assess.* 191 (415) <https://doi.org/10.1007/s10661-019-7514-0>.
- Lavorel, S., Bayer, A., Bondeau, A., Lautenbach, S., Ruiz-Frau, A., Schulz, N., Seppelt, R., Verburg, P., van Teeffelen, A., Vannier, C., Arneth, A., Cramer, W., Marba, N., 2017. Pathways to bridge the biophysical realism gap in ecosystem services mapping approaches. *Ecol. Indicat.* 74, 241–260. <https://doi.org/10.1016/j.ecolind.2016.11.015>.
- Leyk, S., Gaughan, A.E., Adamo, S.B., de Sherbinin, A., Balk, D., Freire, S., Rose, A., Stevens, F.R., Blankenspoor, B., Frye, C., Comenetz, J., Sorichetta, A., MacManus, K., Pistolesi, L., Levy, M., Tatem, A.J., Pesaresi, M., 2019. The spatial allocation of population: a review of large-scale gridded population data products and their fitness for use. *Earth Syst. Sci. Data* 11, 1385–1409. <https://doi.org/10.5194/essd-11-1385-2019>.
- Lillesand, T., Kiefer, R.W., Chipman, J., 2015. *Remote Sensing and Image Interpretation*. John Wiley & Sons.
- Lin, Q., Yu, S., 2018. Losses of natural coastal wetlands by land conversion and ecological degradation in the urbanizing Chinese coast. *Sci. Rep.* 8, 15046 <https://doi.org/10.1038/s41598-018-33406-x>.
- Liu, W., Zhan, J., Zhao, F., Yan, H., Zhang, F., Wei, X., 2019. Impacts of urbanization-induced land-use changes on ecosystem services: a case study of the Pearl River Delta Metropolitan Region, China. *Ecol. Indicat.* 98, 228–238. <https://doi.org/10.1016/j.ecolind.2018.10.054>.
- Lolu, A.J., Ahluwalia, A.S., Sidhu, M.C., Reshi, Z.A., Mandotra, S.K., 2020. Carbon Sequestration and Storage by Wetlands: Implications in the Climate Change Scenario. In: *Restoration of Wetland Ecosystem: A Trajectory towards a Sustainable Environment*. Springer, Singapore, pp. 45–58. <https://doi.org/10.1007/978-981-13-7665-8-4>.
- Lone, S.A., Mayer, I.A., 2019. Geo-spatial analysis of land use/land cover change and its impact on the food security in District Anantnag of Kashmir Valley. *GeoJournal* 84, 785–794. <https://doi.org/10.1007/s10708-018-9891-2>.
- Malik, M.I., 2012. Analysis of population growth and land use change in Anantnag town of South Kashmir using remote sensing and geographical information system. *J. Exp. Sci.* 3, 23–27. <https://core.ac.uk/download/pdf/236016521.pdf>.
- Malik, M.M., Tali, J.A., Nasrath, A., 2017. Assessment of land use and land cover change in district Baramulla, Jammu and Kashmir. *Res. Rev.* 6 (3), 1–14. <https://doi.org/10.37591/v6i3.92>.
- Mantyka-pringle, C.S., Martin, T.G., Rhodes, J.R., 2012. Interactions between climate and habitat loss effects on biodiversity: a systematic review and meta-analysis. *Global Change Biol.* 18, 1239–1252. <https://doi.org/10.1111/j.1365-2486.2011.02593.x>.
- Mao, D., Wang, Z., Wu, J., Wu, B., Zeng, Y., Song, K., Luo, L., 2018. China's wetlands loss to urban expansion. *Land Degrad. Dev.* 29, 2644–2657. <https://doi.org/10.1002/ldr.2939>.
- Meraj, G., Farooq, M., Singh, S.K., Islam, M., Kanga, S., 2022. Modeling the sediment retention and ecosystem provisioning services in the Kashmir valley, India, Western Himalayas. *Modeling Earth Syst. Environ.* 8, 3859–3884. <https://doi.org/10.1007/s40808-021-01333-y>.
- Mitasova, H., Brown, W.M., Hohmann, M., Warren, S., 2001. Geographic Modeling Systems Laboratory. In: *Using Soil Erosion Modeling for Improved Conservation Planning: a GIS-Based Tutorial*. University of Illinois at Urbana-Champaign, Champaign, IL. http://fatra.cnr.ncsu.edu/~hmitasov/gmslab/reports/CerlErosionTutorial/denix/Data/deriving_erosion_modeling_inputs.htm.
- Mouri, G., Takizawa, S., Oki, T., 2011. Spatial and temporal variation in nutrient parameters in stream water in a rural-urban catchment, Shikoku, Japan: effects of land cover and human impact. *J. Environ. Manag.* 92, 1837–1848. <https://doi.org/10.1016/j.jenvman.2011.03.005>.
- Mushtaq, F., Lala, Nee, , M. G., Mantoo, A.G., 2022. Trophic state assessment of a freshwater Himalayan lake using Landsat 8 OLI satellite imagery: a case study of Wular Lake, Jammu and Kashmir (India). *Earth Space Sci.* 9 <https://doi.org/10.1029/2021EA001653> e2021EA001653.

- Nengroo, Z.A., Bhat, M.S., Kuchay, N.A., 2017. Measuring urban sprawl of Srinagar city, Jammu and Kashmir, India. *Journal of Urban Management* 6, 45–55. <https://doi.org/10.1016/j.jum.2017.08.001>.
- OECD (Organization for Economic Cooperation and Development), 1982.** Eutrophication of waters, monitoring, assessment and control, Final report OECD cooperative programme on monitoring of inland waters (eutrophication control) (154), 154. Environment Directorate, OECD, Paris.
- Pan, J., Wen, Y., 2014. Estimation of soil erosion using RUSLE in Caijiamiao watershed, China. *Nat. Hazards* 71 (3), 2187–2205. <https://doi.org/10.1007/s11069-013-1006-2>.
- Panagos, P., Meusburger, K., Ballabio, C., Borrelli, P., Alewell, C., 2014. Soil erodibility in Europe: a high-resolution dataset based on LUCAS. *Sci. Total Environ.* 479, 189–200. <https://doi.org/10.1016/j.scitotenv.2014.02.010>.
- Panagos, P., Borrelli, P., Meusburger, K., Alewell, C., Lugato, E., Montanarella, L., 2015. Estimating the soil erosion cover-management factor at the European scale. *Land Use Pol.* 48, 38–50. <https://doi.org/10.1016/j.landusepol.2015.05.021>.
- Pandit, A.K., 1988. Threats to Kashmir wetlands and their wildlife resources. *Environ. Conserv.* 15, 266–268. <https://doi.org/10.1017/S0376892900029441>.
- Pandit, A.K., 1991. Conservation of wildlife resources in wetland ecosystems of Kashmir, India. *J. Environ. Manag.* 33, 143–154. [https://doi.org/10.1016/S0301-4797\(05\)80090-8](https://doi.org/10.1016/S0301-4797(05)80090-8).
- Pandit, M.K., Sodhi, N.S., Koh, L.P., Bhaskar, A., Brook, B.W., 2007. Unreported yet massive deforestation driving loss of endemic biodiversity in Indian Himalaya. *Biodivers. Conserv.* 16, 153–163. <https://doi.org/10.1007/s10531-006-9038-5>.
- Parry, S.Y., Koul, B., 2020. Water, Soil & Aquatic Diversity of Chatlam wetland. EduBubs Publishing House, Lucknow India.
- Parry, S.Y., Ahmad, S., Zubair, S.M., 2010. Limnological profile of a sub urban wetland, Chatlam, Kashmir. *Int. J. Lakes Rivers (IJLR)* 3, 1–6.
- Parvez, S., Bhat, S.U., 2014. Searching for water quality improvement in Dal lake, Srinagar, Kashmir. *J. Himalayan Ecol. Sustain.* Dev. 9, 51–64. <http://envirsc.uok.edu.in/Files/ablac1fl-07e3-42a2-85bc-83717ef39155/Journal/0f7e8ec3-3997-4af6-b6f5-9cd55b18fd3b.pdf>.
- Patil, R.J., Sharma, S.K., Tignath, S., 2015. Remote sensing and GIS based soil erosion assessment from an agricultural watershed. *Arabian J. Geosci.* 8, 6967–6984. <https://doi.org/10.1007/s12517-014-1718-y>.
- Pengra, B.W., Stehman, S.V., Horton, J.A., Dockter, D.J., Schroeder, T.A., Yang, Z., Cohen, W.B., Healey, S.P., Loveland, T.R., 2020. Quality control and assessment of interpreter consistency of annual land cover reference data in an operational national monitoring program. *Remote Sens. Environ.* 238 (111261) <https://doi.org/10.1016/j.rse.2019.111261>.
- Penny, G., Dar, Z.A., Müller, M.F., 2022. Climatic and anthropogenic drivers of a drying Himalayan river. *Hydroclim. Earth Syst. Sci.* 26, 375–395. <https://doi.org/10.5194/hess-26-375-2022>.
- Phinzi, K., Ngatar, N.S., 2019. The assessment of water-borne erosion at catchment level using GIS-based RUSLE and remote sensing: a review. *Int. Soil Water Conserv. Res.* 7, 27–46. <https://doi.org/10.1016/j.iswcr.2018.12.002>.
- Polgar, G., Jaafer, Z., 2018. Endangered forested wetlands of Sundaland. Springer Berlin Heidelberg 89–93.
- Pratihast, A.K., DeVries, B., Avitabile, V., De Bruin, S., Herold, M., Bergsma, A., 2016. Design and implementation of an interactive web-based near real-time forest monitoring system. *PLoS One* 11, e0150935. <https://doi.org/10.1371/journal.pone.0150935>.
- Qiao, X., Gu, Y., Zou, C., Xu, D., Wang, L., Ye, X., Huang, X., 2019. Temporal variation and spatial scale dependency of the trade-offs and synergies among multiple ecosystem services in the Taihu Lake Basin of China. *Sci. Total Environ.* 651, 218–229. <https://doi.org/10.1016/j.scitotenv.2018.09.135>.
- Rafiq, M., Mishra, A.K., Meer, M.S., 2018. On land-use and land-cover changes over Lidder Valley in changing environment. *Spatial Sci.* 24, 275–285. <https://doi.org/10.1080/19475683.2018.1520300>.
- Raina, R., 1981. Plankton Dynamics and Hydrobiology of Bodsar Lake, Kashmir (Ph. D. Thesis (Unpublished)). University of Kashmir.
- Raina, R., Wanganeo, A., Fozia, S., Pramod, K., 2009. Variation in summer Limnological characteristics of Bodsar wetland over a period of more than two decades. *J. Himalayan Ecol. Sustain. Dev.* 4, 9–21.
- Rashid, I., Aneaus, S., 2019. High-resolution earth observation data for assessing the impact of land system changes on wetland health in Kashmir Himalaya, India. *Arabian J. Geosci.* 12 (453) <https://doi.org/10.1007/s12517-019-4649-9>.
- Rashid, I., Farooq, M., Muslim, M., Romshoo, S.A., 2013. Assessing the impact of anthropogenic activities on 518 Manasbal Lake in Kashmir Himalayas. *Int. J. Environ. Sci.* 3, 2036–2047.
- Rashid, I., Romshoo, S.A., Chaturvedi, R.K., Ravindranath, N.H., Sukumar, R., Jayaraman, M., Sharma, J., 2015. Projected climate change impacts on vegetation distribution over Kashmir Himalayas. *Climatic Change* 132, 601–613. <https://doi.org/10.1007/s10584-015-1456-5>.
- Rashid, I., Romshoo, S.A., Hajam, J.A., Abdullah, T., 2016. A semi-automated approach for mapping geomorphology in mountainous terrain, Ferrozpora watershed (Kashmir Himalaya). *J. Geol. Soc. India* 88, 206–212. <https://doi.org/10.1007/s12594-016-0479-5>.
- Rashid, I., Bhat, M.A., Romshoo, S.A., 2017a. Assessing changes in the above ground biomass and carbon stocks of Lidder valley, Kashmir Himalaya, India. *Geocarto Int.* 32, 717–734. <https://doi.org/10.1080/10106049.2016.1188164>.
- Rashid, I., Romshoo, S.A., Amin, M., Khanday, S.A., Chauhan, P., 2017b. Linking human-biophysical interactions with the trophic status of Dal Lake, Kashmir Himalaya, India. *Limnologica* 62, 84–96. <https://doi.org/10.1016/j.limno.2016.11.008>.
- Rashid, I., Majeed, U., Aneaus, S., Pelto, M., 2020. Linking the recent glacier retreat and depleting streamflow patterns with land system changes in Kashmir Himalaya, India. *Water* 12 (1168). <https://doi.org/10.3390/w12041168>.
- Rashid, I., Dar, S.A., Bhat, S.U., 2022a. Modelling the hydrological response to urban land-use changes in three Wetland catchments of the Western Himalayan region. *Wetlands* 42 (64). <https://doi.org/10.1007/s13157-022-01593-z>.
- Rashid, I., Bhat, I.A., Najar, N.A., Kang, S., Jan, F.Z., Dar, S.A., Bhat, S.U., Kashani, S.D. R., Rasool, W., 2022b. Aerosol variability and glacial chemistry over the western Himalayas. *Environ. Chem.* 15, 312–327. <https://doi.org/10.1071/EN22022>.
- Rasool, R., Fayaz, A., ul Shafiq, M., Singh, H., Ahmed, P., 2021. Land use land cover change in Kashmir Himalaya: linking remote sensing with an indicator based DPSIR approach. *Ecol. Indicat.* 125, 107447 <https://doi.org/10.1016/j.ecolind.2021.107447>.
- Rather, S.A., Pandit, A.K., 2002. Phytoplankton dynamics in Hokarsar wetland, Kashmir. *Int. Soil Water Conserv. Res.* 2, 25–46.
- Rather, M.I., Rashid, I., Shahi, N., Murtaza, K.O., Hassan, K., Yousuf, A.R., Romshoo, S. A., Shah, I.Y., 2016. Massive land system changes impact water quality of the Jhelum River in Kashmir Himalaya. *Environ. Monit. Assess.* 188 (185) <https://doi.org/10.1007/s10661-016-5190-x>.
- Reddy, C.S., Sreelekshmi, S., Jha, C.S., Dadhwali, V.K., 2013. National assessment of forest fragmentation in India: landscape indices as measures of the effects of fragmentation and forest cover change. *Ecol. Eng.* 60, 453–464. <https://doi.org/10.1016/j.ecoleng.2013.09.064>.
- Renard, K.G., Foster, G.R., Weesies, G.A., McCool, D.K., Yoder, D.C., 1997. Predicting soil erosion by water: a guide to conservation planning with the revised universal soil loss equation (RUSLE). Agriculture Handbook Number 703, Agricultural Research Service, United States Department of Agriculture. <https://naldc.nal.usda.gov/download/11126/PDF>.
- Romshoo, S.A., Rashid, I., 2014. Assessing the impacts of changing land cover and climate on Hokarsar wetland in Indian Himalayas. *Arabian J. Geosci.* 7 (1), 143–160. <https://doi.org/10.1007/s12517-012-0761-9>.
- Romshoo, S.A., Bhat, S.A., Rashid, I., 2012. Geoinformatics for assessing the morphometric control on hydrological response at watershed scale in the Upper Indus Basin. *J. Earth Syst. Sci.* 121, 659–686. <https://doi.org/10.1007/s12040-012-0192-8>.
- Romshoo, S.A., Altaf, S., Rashid, I., Dar, R.A., 2018. Climatic, geomorphic and anthropogenic drivers of the 2014 extreme flooding in the Jhelum basin of Kashmir, India. *Geomatics, Natural Hazards and Risk* 9, 224–248. <https://doi.org/10.1080/19475705.2017.1417332>.
- Sahana, M., Hong, H., Sajjad, H., 2018. Analyzing urban spatial patterns and trend of urban growth using urban sprawl matrix: a study on Kolkata urban agglomeration, India. *Sci. Total Environ.* 628–629, 1557–1566. <https://doi.org/10.1016/j.scitotenv.2018.02.170>.
- Sajjad, H., Iqbal, M., 2012. Impact of urbanization on land use/land cover of Dudhganga watershed of Kashmir Valley, India. *Int. J. Urban Sci.* 16, 321–339. <https://doi.org/10.1080/12265934.2012.743749>.
- Saraswat, C., Kumar, P., Mishra, B.K., 2016. Assessment of stormwater runoff management practices and governance under climate change and urbanization: an analysis of Bangkok, Hanoi and Tokyo. *Environ. Sci. Pol.* 64, 101–117. <https://doi.org/10.1016/j.envsci.2016.06.018>.
- Saumer, P., Schonbrodt, S., Behrens, T., Seeber, C., Scholten, T., 2010. Assessing the USLE crop and management factor C for soil erosion modeling in a large mountainous watershed in Central China. *J. Earth Sci.* 21, 835–845. <https://doi.org/10.1007/s12583-010-0135-8>.
- Schmiegelow, F.K., Mönkkönen, M., 2002. Habitat loss and fragmentation in dynamic landscapes: avian perspectives from the boreal forest. *Ecol. Appl.* 12, 375–389. [https://doi.org/10.1890/1051-0761\(2002\)012\[0375:HAFID\]2.0.CO;2](https://doi.org/10.1890/1051-0761(2002)012[0375:HAFID]2.0.CO;2).
- Shah, J.A., Pandit, A.K., Shah, G.M., 2021. Zooplankton Community: A Valuable Bio-Indicator Tool in Disturbed Wetlands in Freshwater Pollution and Aquatic Ecosystems. Apple Academic Press, pp. 205–240.
- Shaheen, H., Mushtaq, A., Khan, R.W.A., Azad, B., 2016. Fuelwood consumption pattern and its impact on forest structure in Kashmir Himalayas. *Bosque* 37, 419–424. <https://doi.org/10.4067/S0717-92002016000200020>.
- Shaheen, H., Awan, S.N., Aziz, S., 2017. Distribution pattern, conservation status, and associated flora of the genus Juniperus in subalpine pastures of the Kashmir Himalayas. *Mt. Res. Dev.* 37, 487–493. <https://doi.org/10.1659/MRD-JOURNAL-D-16-00119.1>.
- Sharma, A., Tiwari, K.N., Bhadoria, P.B.S., 2011. Effect of land use land cover change on soil erosion potential in an agricultural watershed. *Environ. Monit. Assess.* 173, 789–801. <https://doi.org/10.1007/s10661-010-1423-6>.
- Sheikh, A., Palria, H.S., Alam, A., 2011. Integration of GIS and universal soil loss equation (USLE) for soil loss estimation in a Himalayan watershed. *Recent Res. Sci. Technol.* 3, 51–57.
- Shen, G., Yang, X., Jin, Y., Xu, B., Zhou, Q., 2019. Remote sensing and evaluation of the wetland ecological degradation process of the Zoige Plateau Wetland in China. *Ecol. Indicat.* 104, 48–58. <https://doi.org/10.1016/j.ecolind.2019.04.063>.
- Showqi, I., Rashid, I., Romshoo, S.A., 2014. Land use land cover dynamics as a function of changing demography and hydrology. *GeoJournal* 79, 297–307. <https://doi.org/10.1007/s10708-013-9494-x>.
- Showqi, I., Lone, F.A., Naikoo, M., 2018. Preliminary assessment of heavy metals in water, sediment and macrophyte (*Lemna minor*) collected from Anchar Lake, Kashmir, India. *Appl. Water Sci.* 8 (80) <https://doi.org/10.1007/s13201-018-0720-z>.
- Shrestha, D.P., Jetten, V.G., 2018. Modelling erosion on a daily basis, an adaptation of the MMF approach. *Int. J. Appl. Earth Obs. Geoinf.* 64, 117–131. <https://doi.org/10.1016/j.jag.2017.09.003>.

- Shrestha, M.K., York, A.M., Boone, C.G., Zhang, S., 2012. Land fragmentation due to rapid urbanization in the Phoenix Metropolitan Area: Analyzing the spatiotemporal patterns and drivers. *Appl. Geogr.* 32, 522–531. <https://doi.org/10.1016/j.apgeog.2011.04.004>.
- Singh, M., Sinha, R., 2021. Hydrogeomorphic indicators of wetland health inferred from multi-temporal remote sensing data for a new Ramsar site (Kaabar Tal), India. *Ecol. Indicat.* 127, 107739. <https://doi.org/10.1016/j.ecolind.2021.107739>.
- Singh, G., Chandra, S., Babu, R., 1981. Soil loss and prediction research in India, central soil and water conservation research training institute. Bulletin No T-12 D 9 (1981). <https://agris.fao.org/agris-search/search.do?recordID=US201300006468>.
- Smol, J.P., Wolfe, A.P., Birks, H.J.B., Douglas, M.S., Jones, V.J., Korholo, A., Weckström, J., 2005. Climate-driven regime shifts in the biological communities of arctic lakes. *Proc. Natl. Acad. Sci. USA* 102, 4397–4402. <https://doi.org/10.1073/pnas.0500245102>.
- Song, K., Choi, Y.E., Han, H.J., Chon, J., 2021. Adaptation and transformation planning for resilient social-ecological system in coastal wetland using spatial-temporal simulation. *Sci. Total Environ.* 789, 148007. <https://doi.org/10.1016/j.scitotenv.2021.148007>.
- Stone, R.P., 2012. Universal soil loss equation (USLE) factsheet. ISSN. Ontario ministry of Agriculture, Food and Rural Affairs (OMAFRA). pp. 1198–1712.
- Stone, R.P., Hilborn, D., 2000. Universal soil loss equation (USLE). Ontario Ministry of Agriculture, Food and Rural Affairs Factsheet.
- Sui, X., Zhang, R., Frey, B., Yang, L., Li, M.H., Ni, H., 2019. Land use change effects on diversity of soil bacterial, Acidobacterial and fungal communities in wetlands of the Sanjiang Plain, northeastern China. *Sci. Rep.* 9, 18535. <https://doi.org/10.1038/s41598-019-55063-4>.
- Sun, R., Yao, P., Wang, W., Yue, B., Liu, G., 2017. Assessment of wetland ecosystem health in the Yangtze and Amazon river Basins. *ISPRS Int. J. Geo-Inf.* 6 (81) <https://doi.org/10.3390/ijgi6030081>.
- Varshney, A., 1991. India, Pakistan, and Kashmir: antinomies of nationalism. *Asian Surv.* 31, 997–1019. <https://doi.org/10.2307/2645304>.
- Vass, K.K., Wangeneo, A., Samanta, S., Adhikari, S., Muralidhar, M., 2015. Phosphorus dynamics, eutrophication and fisheries in the aquatic ecosystems in India. *Curr. Sci.* 108, 1306–1314.
- Vega, C., Pertierri, G., Olalla-Tárraga, L.R., M. Á, 2017. MERRAclim, a high-resolution global dataset of remotely sensed bioclimatic variables for ecological modelling. *Sci. Data* 4, 170078. <https://doi.org/10.1038/sdata.2017.78>.
- Verhoeven, J.T., Setter, T.L., 2010. Agricultural use of wetlands: opportunities and limitations. *Ann. Bot.* 105, 155–163. <https://doi.org/10.1093/aob/mcp172>.
- Wanda, E.M., Mamba, B.B., Msagati, T.A., Msilimba, G., 2016. Determination of the health of Lunyangwa wetland using wetland classification and risk assessment index. *Physics and chemistry of the earth. Parts A/B/C* 92, 52–60. <https://doi.org/10.1016/j.pce.2015.09.010>.
- Wang, G., Liu, J., Kubota, J., Chen, L., 2007. Effects of land-use changes on hydrological processes in the middle basin of the Heihe River, northwest China. *Hydrol. Process.* 21, 1370–1382. <https://doi.org/10.1002/hyp.6308>.
- Wang, L.Y., Xiao, Y., Rao, E.M., Jiang, L., Xiao, Y., Ouyang, Z.Y., 2018. An assessment of the impact of urbanization on soil erosion in Inner Mongolia. *Int. J. Environ. Res. Publ. Health* 15 (550). <https://doi.org/10.3390/ijerph15030550>.
- Wu, F., Zhan, J., Xu, Q., Xiong, Y., Sun, Z., 2013. A comparison of two land use simulation models under the RCP4. 5 Scenario in China. *Adv. Meteorol.* 578350 <https://doi.org/10.1155/2013/578350>.
- Xu, C., Xu, Z., Yang, Z., 2020. Reservoir operation optimization for balancing hydropower generation and biodiversity conservation in a downstream wetland. *J. Clean. Prod.* 245, 118885. <https://doi.org/10.1016/j.jclepro.2019.118885>.
- Yousuf, A., Romshoo, S.A., 2022. Impact of land system changes and extreme precipitation on peak flood discharge and sediment yield in the upper Jhelum Basin, Kashmir Himalaya. *Sustainability* 14, 13602. <https://doi.org/10.3390/su142013602>.
- Zaz, S.N., Romshoo, S.A., 2012. Assessing the geoindicators of land degradation in the Kashmir Himalayan region, India. *Nat. Hazards* 64, 1219–1245. <https://doi.org/10.1007/s11069-012-0293-3>.
- Zedler, J.B., Kercher, S., 2005. Wetland resources: status, trends, ecosystem services, and restorability. *Annu. Rev. Environ. Resour.* 30, 39–74. <https://doi.org/10.1146/annurev.energy.30.050504.144248>.
- Zhang, H., Yang, Q., Li, R., Liu, Q., Moore, D., He, P., Ritsema, C.J., Geissen, V., 2013. Extension of a GIS procedure for calculating the RUSLE equation LS factor. *Comput. Geosci.* 52, 177–188. <https://doi.org/10.1016/j.cageo.2012.09.027>.
- Zhao, B., Li, B., Zhong, Y., Nakagoshi, N., Chen, J.K., 2005. Estimation of ecological service values of wetlands in Shanghai, China. *Chin. Geogr. Sci.* 15, 151–156. <https://doi.org/10.1007/s11769-005-0008-8>.